DEVELOPMENT OF CATALYSTS FOR BIOMASS TRANSFORMATION

M.Sc. Thesis

By

SNEHA SINGH



Supervised by: Prof. Sanjay K. Singh

DEPARTMENT OF CHEMISTRY INDIAN INSTITUTE OF TECHNOLOGY INDORE MAY 2025

DEVELOPMENT OF CATALYSTS FOR BIOMASS TRANSFORMATION

A THESIS

Submitted in partial fulfillment of the requirements for the award of the degree of

Master of Science

By
SNEHA SINGH



DEPARTMENT OF CHEMISTRY INDIAN INSTITUTE OF TECHNOLOGY INDORE MAY 2025



INDIAN INSTITUTE TECHNOLOGY INDORE

OF

CANDIDATE'S DECLARATION

I hereby certify that the work which is being presented in the thesis entitled "Development of catalysts for biomass transformation" in the partial fulfillment of the requirements for the award of the degree of Master of Science and submitted in the Department of Chemistry, Indian Institute of Technology Indore, is an authentic record of my own work carried out during the time period from July 2024 to May 2025 under the supervision of Prof. Sanjay Kumar Singh.

The matter presented in this thesis has not been submitted by me for the award of any other degree of this or any other institute.

Sneha Singh

This is to certify that the above statement made by the candidate is correct to the best of my knowledge.

Signature of the Supervisor of M.Sc. thesis

(Prof. Sanjay K. Singh)

Sneha Singh has successfully given her M.Sc. Oral Examination held on May 2025.

Signature of Supervisor of MSc thesis

Prof. Sanjay K. Singh

Date:

ACKNOWLEDGEMENTS

- I want to thank Prof. Sanjay Kumar Singh, my M.Sc. supervisor, for being a constant source of support and guidance during this time. He always encouraged me to think independently and supported my ideas as I explored the field of heterogeneous catalysts for hydrogenation. He made sure I felt comfortable and encouraged me to learn new things, whether it was about lab equipment or new skills. He created an environment where I felt free to share any problems or concerns, I had, which helped me grow both personally and academically. Overall, his support and encouragement have been invaluable to my journey.
- I would also like to thank SIC, IIT Indore, for providing all the needed instrumentation facilities. I would also like to thank DST-FIST 500 MHz NMR facility, Department of Chemistry, for the NMR facility.
- In coursework during my M.Sc. first year, I learnt a lot. I would like to thank all the faculty members of the Department of Chemistry. I am very grateful to Dr. Tushar Kanti Mukherjee (HoD, Department of Chemistry) and Dr. Umesh A. Kshirsagar (DPGC, Department of Chemistry) for their support. The Chemistry office staff members deserve special thanks. They are always ready to help and personally take care of any problem or task.
- I thank my group members, Dr. Pooja Prajapati, Mr. Tushar Ashok Kharde, Ms. Jayashree Parthiban, Mr. Khanindra Kalita, Mr. Kanhaiya Singh, Mr. Shivam Mishra, Ms. Aditi Gautam, and Ms. Pallvi Sharma, for their constant support. They have always helped me with learning new methodologies and laboratory techniques and solved my laboratory-related queries.
- Finally, I want to express my heartfelt gratitude to my parents for their unwavering support and unshakeable faith in me. They have been my pillars of strength, always encouraging me and granting me the freedom to pursue my dreams. Without their support, I would never have made it this far.

Dedicated to my parents

Abstract

Biomass is a composition of cellulose, lignin, and hemicellulose. Cellulose and lignin serve as key precursors for the synthesis of a wide range of value-added chemicals and fuels. This project involves the extraction and separation of lignin and cellulose from biomass sources, specifically wheat straw, wood dust, and rice straw. Following separation, we will decompose the lignin into various monophenolic compounds, including syringaldehyde, hydroxybenzaldehyde. The generated aldehydic compounds will undergo condensation reactions with ketones to produce substrates with an elevated carbon count. In this thesis, we aim to employ various catalytic processes to facilitate hydrogenation and hydrodeoxygenation of these substrates. The focus is to convert these compounds into hydrocarbons that meet the specifications for jet fuel applications. This thesis comprises four chapters, structured as follows: The first chapter deals with the general introduction of the extraction of lignin and cellulose from lignocellulosic biomass. The second chapter includes the experimental procedures adopted for catalyst synthesis, substrate synthesis, and the execution of various catalytic reactions. The third chapter includes a detailed discussion of the results obtained from various substrate synthesis and hydrogenation experiments. The final chapter presents the conclusion of the thesis, highlighting the major findings. The primary goal of this thesis is to develop an active and efficient heterogeneous catalyst that operates under environmentally benign conditions for biomass transformation.

TABLE OF CONTENTS

- 1. LIST OF FIGURES
- 2. LIST OF TABLES
- 3. LIST OF SCHEMES
- 4. ACRONYMS
- 5. NOMENCLATURE

Chapter 1: Introduction

- 1.1 General introduction
- 1.2 Literature review and problem formulation
- **1.3** Objective of the project

Chapter 2: Experimental section

- **2.1** Materials and instrumentation
- 2.2 Synthesis of Ru nanoparticles
- **2.3** Extraction of cellulose and lignin from wheat straw
- **2.4** Synthesis of substrates
- 2.4.1 Synthesis of 2,6-dibenzylcyclohexan-1-one
- 2.4.2 Synthesis of chalcone
- 2.4.3 Synthesis of (E)-1-phenyl-3-(o-tolyl) prop-2-en-1-one
- 2.4.4 Synthesis of (E)-1-phenyl-3-(m-tolyl) prop-2-en-1-one
- 2.4.5 Synthesis of (E)-1-phenyl-3-(p-tolyl) prop-2-en-1-one
- 2.4.6 Synthesis of (E)-4-phenylbut-3-en-2-one
- 2.4.7 Synthesis of (1E,4E)-1,5-diphenylpenta-1,4-dien-3-one
- 2.4.8 Synthesis of (1E,4E)-1,5-di-p-tolylpenta-1,4-dien-3-one
- **2.5** Catalytic hydrogenation reactions
- 2.5.1 Hydrogenation reaction of (E)-1-phenyl-3-(p-tolyl) prop-2-en-1-one

- 2.5.2 Hydrogenation reaction of (E)-1-phenyl-3-(o-tolyl) prop-2-en-1-one
- 2.5.3 Hydrogenation reaction of chalcone

Chapter 3: Results and discussion

- **3.1** Characterization of the Ru nanoparticles
- 3.2 Characterization of lignin
- **3.3** Characterization of 2,6-dibenzylcyclohexan-1-one
- **3.4** Characterization of chalcone
- **3.5** Characterization of (E)-1-phenyl-3-(*o*-tolyl) prop-2-en-1-one
- **3.6** Characterization of (E)-1-phenyl-3-(*m*-tolyl) prop-2-en-1-one
- **3.7** Characterization of (E)-1-phenyl-3-(*p*-tolyl) prop-2-en-1-one
- **3.8** Characterization of (E)-4-phenylbut-3-en-2-one
- **3.9** Characterization of (1E,4E)-1,5-diphenylpenta-1,4-dien-3-one
- **3.10** Characterization of (1E,4E)-1,5-di-*p*-tolylpenta-1,4-dien-3-one
- **3.11** Hydrogenation reaction of (E)-1-phenyl-3-(p-tolyl) prop-2-en-1-one
- **3.12** Hydrogenation reaction of (E)-1-phenyl-3-(o-tolyl) prop-2-en-1-one
- **3.13** Hydrogenation reaction of chalcone

Chapter 4: Conclusions and Scope of Work REFERENCES

LIST OF FIGURES

- **Figure 1:** P-XRD Pattern, SEM image and corresponding EDS spectra of Ru nanoparticles
- Figure 2: FTIR Spectra of wheat straw lignin
- Figure 3: ¹H NMR spectra of 2,6-dibenzylcyclohexan-1-one
- Figure 4: ¹³C NMR spectra of 2,6-dibenzylcyclohexan-1-one
- Figure 5: LCMS Spectra of 2,6-dibenzylcyclohexan-1-one
- Figure 6: ¹H NMR spectra of chalcone
- Figure 7: ¹³C NMR spectra of chalcone
- **Figure 8:** ¹H NMR spectra of (E)-1-phenyl-3-(*o*-tolyl) prop-2-en-1-one
- **Figure 9:** ¹³C NMR spectra of (E)-1-phenyl-3-(*o*-tolyl) prop-2-en-1-one
- **Figure 10:** ¹H NMR spectra of (E)-1-phenyl-3-(*m*-tolyl) prop-2-en-1-one
- Figure 11: ¹³C NMR spectra of (E)-1-phenyl-3-(*m*-tolyl) prop-2-en-1-one
- **Figure 12:** ¹H NMR spectra of (E)-1-phenyl-3-(*p*-tolyl) prop-2-en-1-one
- Figure 13: ¹³C NMR spectra of (E)-1-phenyl-3-(p-tolyl) prop-2-en-1-one
- **Figure 14:** ¹H NMR spectra of (E)-4-phenylbut-3-en-2-one
- Figure 15: ¹³C NMR spectra of (E)-4-phenylbut-3-en-2-one
- Figure 16: ¹H NMR spectra of (1E,4E)-1,5-diphenylpenta-1,4-dien-3-one
- Figure 17: ¹³C NMR spectra of (1E,4E)-1,5-diphenylpenta-1,4-dien-3-one
- Figure 18: ¹H NMR spectra of (1E,4E)-1,5-di-*p*-tolylpenta-1,4-dien-3-one
- Figure 19: ¹³C NMR spectra of (1E,4E)-1,5-di-*p*-tolylpenta-1,4-dien-3-one
- **Figure 20:** ¹H NMR spectra of hydrogenation of (E)-1-phenyl-3-(*p*-tolyl) prop-2-en-1-one for 8 h
- **Figure 21:** ¹H NMR spectra of hydrogenation of (E)-1-phenyl-3-(*p*-tolyl) prop-2-en-1-one for 12 h
- **Figure 22:** Selectivity and conversion for hydrogenation of (E)-1-phenyl-3-(*p*-tolyl) prop-2-en-1-one in different time scales
- **Figure 23:** ¹H NMR spectra of hydrogenation of (E)-1-phenyl-3-(*o*-tolyl) prop-2-en-1-one

Figure 24: ¹H NMR spectra of hydrogenation of chalcone with 1 bar H₂ pressure

Figure 25: ¹H NMR spectra of hydrogenation of chalcone with 2 bar H₂ pressure

Figure 26: ¹H NMR spectra of hydrogenation of chalcone with 4 bar H₂ pressure

Figure 27: Selectivity and conversion for chalcone in different H₂ pressure

LIST OF TABLES

 Table 1: Literature reports on biomass transformation

Table 2: Optimization table for hydrogenation of (E)-1-phenyl-3-(*p*-tolyl) prop-2-en-1-one

Table 3: Optimization table for hydrogenation of chalcone

LIST OF SCHEMES

Scheme 1: Synthesis of 2,6-dibenzylcyclohexan-1-one

Scheme 2: Synthesis of chalcone

Scheme 3: Synthesis of (E)-1-phenyl-3-(*o*-tolyl) prop-2-en-1-one

Scheme 4: Synthesis of (E)-1-phenyl-3-(*m*-tolyl) prop-2-en-1-one

Scheme 5: Synthesis of (E)-1-phenyl-3-(*p*-tolyl) prop-2-en-1-one

Scheme 6: Synthesis of (E)-4-phenylbut-3-en-2-one

Scheme 7: Synthesis of (1E,4E)-1,5-diphenylpenta-1,4-dien-3-one

Scheme 8: Synthesis of (1E,4E)-1,5-di-*p*-tolylpenta-1,4-dien-3-one

Scheme 9: Hydrogenation of (E)-1-phenyl-3-(*p*-tolyl) prop-2-en-1-one for 8 h

Scheme 10: Hydrogenation of (E)-1-phenyl-3-(*p*-tolyl) prop-2-en-1-one for 12 h

Scheme 11: Hydrogenation of (E)-1-phenyl-3-(*o*-tolyl) prop-2-en-1-one

Scheme 12: Hydrogenation of chalcone with 1 bar H₂ pressure

Scheme 13: Hydrogenation of chalcone with 2 bar H₂ pressure

Scheme 14: Hydrogenation of chalcone with 4 bar H₂ pressure

ACRONYMS

CDCl₃ Chloroform-d

CTAB Cetyltrimethylammonium bromide

D₂O Deuterium oxide

FTIR Fourier transform infrared spectroscopy

GC-MS Gas chromatography-mass spectrometry

H₂ Hydrogen

LC-MS Liquid chromatography-mass spectrometry

NMR Nuclear magnetic resonance

NP'S Nanoparticles

P-XRD Powder X-ray diffraction

Ru Ruthenium

RuCl₃. xH₂O Ruthenium (III) chloride hydrate

NaBH₄ Sodium borohydride

TMS Tetramethyl silane

NOMENCLATURE

°C Degree celsius

g Gram

h Hour

mL Milliliter

mmol Millimole

Min Minutes

mg Milligram

RB Round bottom

Ref. Reference

T Temperature

t Time

Chapter 1: Introduction

1.1 General Introduction

The rapid consumption of fossil fuels is driven by overexploitation linked to industrial development and population growth. As a sustainable alternative, lignocellulosic biomass offers an accessible and cost-effective feedstock. The biomass is a composition of cellulose, lignin, and hemicellulose. Cellulose and lignin serve as key precursors for the synthesis of a wide range of valueadded chemicals and fuels. Glucose is a monomer unit of cellulose connected by β -1,4-glucosidic bonds. Cellulose can be hydrolyzed to produce sugars and liquid fuels. There has been an increase in research interest in converting cellulose into glucose, ³ 5-hydroxymethylfurfural (HMF)⁴ in recent years. After cellulose, lignin is the largest prevalent biopolymer, which constitutes 10-25% of lignocellulosic biomass. The lignin is formed from coniferyl, sinapyl, and p-coumaryl monolignols, which are connected by β -O-4 and C-C bonds.⁵ These monolignols form syringyl (S), p-hydroxyphenyl (H), and guaiacyl (G) units in the lignin structure. The degradation of lignin gives aromatic compounds such as syringaldehyde, vanillin, p-hydroxybenzaldehyde, acetosyringone, acetovanillone, syringic acid, and vanillic acid,6 due to its distinctive structure and chemical properties.

Vanillin, derived from lignin, is gaining recognition as a valuable bio-based aromatic precursor for polymer synthesis. A notable example is provided by Miller et al., who reacted vanillin aldehyde (VA) with acetic anhydride to produce acetyldihydroferulic acid. This compound was then polymerized to form poly (dihydroferulic acid), a sustainable polyester. Interestingly, the resulting material exhibits thermal behaviour akin to that of conventional polyethylene terephthalate (PET), underlining the promising future of lignin-based monomers in the design of renewable aromatic polymers.⁷

Lignin is a renewable source in guaiacyl (G) units found in both herbaceous and woody plants.⁸ As such, utilizing lignin as an economical feedstock for guaiacol production presents significant potential, decreasing the use of fossil resources for this crucial chemical. Furthermore, if we extract guaiacol from the lignin, it can produce a greater variety and larger quantity of chemicals.⁹

Guaiacol is a key feedstock to produce numerous high-value chemicals. Harnessing lignin as an inexpensive and renewable feedstock for the targeted production of guaiacol offers significant potential. Lignin is mainly composed of C-O and C-C bonds. 10 Shen, Xiaojun, et al. found that the Lewis acid can efficiently catalyze the production of guaiacol through the conversion of lignin. This catalytic system facilitates the hydrolysis of ether linkages in lignin, vielding the formation of the compound. target The hydrodeoxygenation of guaiacol presents a carbon-negative environmentally sustainable pathway to produce cyclohexanol, a precursor for nylon. The study focused on the porous properties of a ruthenium-based catalyst mounted on affordable hydrochar, examining the effects of various activation methods. The catalyst showed strong selectivity for cleaving Carvl-O bonds under moderate conditions (0.2 MPa H₂, 160 °C for 4 hours).¹¹ Analysis revealed that catalytic performance was influenced by both hydrothermal treatment and alkali activation which influenced its porous structure and ruthenium dispersion. The growing production of metallic ruthenium shows the efficient control of interactions between the active sites and the support material. By using cellulose-based hydrochar to produce nylon precursors, which are derived from guaiacol, exemplifies an efficient and sustainable strategy for biomass resource utilization.¹²

Lignin is a phenol-based biopolymer with higher energy density than cellulose and hemicellulose, making it the most energy-rich part of lignocellulosic biomass. It is also a good source of phenolic bio-oils. However, these bio-oils contain a lot of oxygen and mainly include compounds like phenol, guaiacol, syringol, and their derivatives. To turn them into useful alkane fuels for transportation, a significant amount of oxygen must be removed. Therefore, phenolic compounds are often used as model substances to study bio-oil. Hydrodeoxygenation (HDO) is commonly used to upgrade bio-oils by reducing their oxygen content.¹³

Phenol is the simplest and one of the most extensively studied model compounds derived from lignin-based bio-oils. It can participate in a wide range of chemical transformations, including halogenation, hydrogenation, oxidation, alkylation, carboxylation, esterification, and etherification. Among

these, alkylation of phenol and its derivatives is particularly important for forming carbon–carbon (C–C) bonds, a key step in synthesizing fuel components.¹⁴

The synthesis of high-density jet fuels has recently emerged as a prominent area of research interest. High-density jet fuel can be broadly applied in the field of aircraft, missiles, and rockets. The higher density allows the aircraft to have a bigger payload and longer range with the same tank volume. Aliphatic hydrocarbon fuel with higher density can be obtained by increasing the length of the carbon chain. Aldol condensation is an important method to increase the length of the carbon chain. A benzaldehyde—acetone—benzaldehyde dimer was produced through aldol condensation of benzaldehyde and acetone. Then, C13 and C12 alkanes were synthesized by hydrogenation and hydrodeoxygenation (HDO).¹⁵

1.2 Literature Survey

Straw, particularly wheat straw, is one of the most plentiful and cost-effective biomass resources available globally. It shows promise as an alternative to fossil fuels and chemical feedstocks. In this study, we focused on lignin and cellulose extraction from wheat straw. We employed a two-stage process to isolate high-quality cellulose and lignin. In the first stage, cellulose was separated from lignin and hemicellulose under lower temperature and acidic conditions. The remaining liquid, which contained a small amount of hemicellulose and most of the lignin, underwent further processing in the second stage with higher temperature and higher acidic concentration than the first stage process. ¹⁶

Guaiacol is a crucial raw material for synthesizing a variety of value-added chemicals, including flavors like vanillin and pharmaceuticals such as eugenol, ¹⁷ as well as a plant growth regulator. Currently, guaiacol production primarily relies on catechol methylation, which is a high-cost derivative sourced from fossil fuels, requiring extra methylation agents like methyl chloride and methanol. However, lignin is a renewable source in guaiacyl (G) units found in both herbaceous and woody plants. The Lewis acid catalyst La (OTf)₃ plays an important role in breaking down the ether bonds in lignin, yielding alkyl-guaiacol and syringol products. These alkyl-guaiacol products can be processed to form guaiacol through decarbonization, while alkyl-syringol can be converted to guaiacol via decarbonization and demethoxylation. This approach is notable for its ability to produce guaiacol directly from lignin transformation with high yields.¹⁸

Producing high-quality fuels from biomass-derived platform chemicals presents significant challenges. In 2021, Longlong et al. developed a Pd/C catalyst that effectively transformed dicyclohexylmethane and perhydrofluorene into C13 alkanes, achieving an impressive maximum conversion rate of 10.42 and 75.20, respectively. In 2018, Zhao et al. developed a Pd/C catalyst that effectively transformed (E)-6-(4hydroxyphenyl)-4-oxohex-5-enoic acid. (E)-6-(4-hydroxy-3methoxyphenyl)-4-oxohex-5-enoic (E)-6-(4-hydroxy-3,5acid and

dimethoxyphenyl)-4-oxohex-5-enoic acid into C12 alkanes, achieving an impressive maximum conversion rate of 81%, 87%, 68% respectively.²⁰

Table 1: Literature reports on biomass transformation:

Entry	Substrate	Catalyst	Solvent	Conditions	Product (yield %)	Ref.
1	Ŏ.	Pd/C	Water	180 °C, 6 MPa H ₂ , 10 h	C13 alkanes (10.42)	19
2	НО	Pd/C	Water	180 °C, 6 MPa H ₂ , 10 h	C13 alkanes (75.20)	19
3	НО	Pd/C	Methanol	RT, 0.1 MPa H ₂ , 2 h	C12 alkanes (81)	20
4	НО	Pd/C	Methanol	RT, 0.1 MPa H ₂ , 2 h	C12 alkanes (87)	20
5	HO OH	Pd/C	Methanol	RT, 0.1 MPa H ₂ , 2 h	C12 alkanes (68)	20

1.3 Objective of the project:

- Design and development of catalysts for biomass transformation.
- To extensively characterize the synthesized catalysts using various techniques like P-XRD (Powder X-ray Diffraction), SEM (Scanning Electron Microscopy), and FTIR (Fourier Transform Infrared spectroscopy).
- To investigate the performance of the synthesized catalysts for the biomass transformation under milder reaction conditions.
- To understand and explore the working of many equipment like tubular furnace, programmable oven, vacuum oven, high-pressure reactors, and other characterization techniques like P-XRD, GC-MS, and elemental analysis. The working principle and handling of these instruments will be learned throughout the year.

Chapter 2: Experimental section

2.1 Material and Instrumentation: All solvents and

reagents for the analysis and synthesis were obtained from Merck, Sigma Aldrich, and TCI. Used as received without any additional purifications. ¹H NMR was recorded in deuterated solvent (CDCl₃, D₂O) using Bruker Advance 400 and Bruker Ascend 500. FTIR was conducted in the mid-IR range spanning from 500 to 4000 cm⁻¹ using the Brucker VERTEX 70 instrument. The P-XRD was performed in Rigaku SmartLab, Automated Multipurpose X-ray Diffractometer. The accurate mass was measured with the help of BRUKER micrOTOF-QII mass spectrometer coupled with Daltonik Ultimate 3000 HPLC.

2.2 Synthesis of Ru nanoparticles:

Ruthenium (III) chloride (0.04 mmol) and CTAB (50 mg) dissolved in water (5 mL) were added dropwise to an aqueous solution of sodium borohydride (25 mg in 5 mL water) to obtain a black suspension of ruthenium nanoparticles. The content of the flask was sonicated for 20 minutes at room temperature to obtain the ruthenium nanoparticles as a black suspension. Ruthenium nanoparticles were collected by centrifugation, washed several times with distilled water, and then dried under vacuum and further used for catalytic reactions.

2.3 Extraction of cellulose and lignin from wheat straw:

The wheat straw (15 g) was first washed with hot water and placed in a vacuum oven at 50 °C for 10 h. After drying, the wheat straw was ground into a powder using a grinder. The powdered wheat straw was sifted through a sieve to collect the powder of different mesh sizes. A total of 11.17 g of the powdered wheat straw was subjected to Soxhlet extraction using 150 mL of a toluene-ethanol (2:1 v/v) mixture for 24 h to remove pigments, oils and wax. After extraction, the powder was oven-dried at 50 °C, resulting in 11.05 g of extracted wheat

straw (EWS). Next, 11.05 g of EWS was combined with 150 mL of a 1,4-dioxane and H₂O (2:1 v/v) mixture, and sulfuric acid was added to a 200 mL stainless steel autoclave. The mixture was heated for 6 h at 150 °C under magnetic stirring with 1 wt% H₂SO₄. The solid residue was then isolated by suction filtration, washed three times with 30 mL of a 1,4-dioxane and H₂O (2:1 v/v) mixture, and dried for 12 h at 70 °C, yielding 1.39 g of wheat straw cellulose. Following this, 300 mL of the filtrate and washes were combined, and H₂SO₄ was added to adjust the concentration to 1.5 wt%. The mixture was then heated at 180 °C for 1.5 h under stirring. After cooling to room temperature, the mixture was transferred to a 1000 mL beaker, and 540 mL of water was added. Lignin precipitated and was collected by filtration, vacuum-dried for 10 h at 70 °C, resulting in 2.3 g of lignin.

2.4 Synthesis of substrates:

2.4.1 Synthesis of 2,6-dibenzylcyclohexan-1-one:

Benzaldehyde (4.918 mmol, 500 μ L) and 1.1 equivalents of K₂CO₃ (5.41 mmol, 747.68 mg) were added to the ethanol (10 mL) and cyclohexanone (5.41 mmol, 560.6 μ L) solution. The reaction mixture was heated to 50 °C for 24 h in an oil bath. Ethanol was evaporated under reduced pressure. Ethyl acetate was used to extract the mixture, and the organic layer was dried over anhydrous Na₂SO₄. After removing all volatiles under reduced pressure, 235.8 mg of a yellow-coloured product was obtained with a 35% yield.

Benzaldehyde (4.92 mmol) (500
$$\mu$$
L) (560.6 μ L) (500 μ L) (500

Scheme 1: Synthesis of 2,6-dibenzylcyclohexan-1-one

2.4.2 Synthesis of chalcone:

A solution of KOH (1 g) in 10 mL distilled water was added dropwise to the stirring solution of acetophenone (1 mmol, 117 μ L) and benzaldehyde (1 mmol, 102 μ L) in ethanol (10 mL) in ice bath for 6 hours. The reaction mixture was extracted using ethyl acetate and dried over Na₂SO₄. The solvent was removed using a rotary evaporator. Yellow solid product was obtained with 77 % yield.

Scheme 2: Synthesis of chalcone

2.4.3 Synthesis of (E)-1-phenyl-3-(o-tolyl) prop-2-en-1-one:

A solution of KOH (1 g) in 10 mL distilled water was added dropwise to the stirring solution of acetophenone (1 mmol, 117 μ L) and *o*-tolualdehyde (1 mmol, 116 μ L) in ethanol (10 mL) in ice bath for 6 hours. The reaction mixture was extracted using ethyl acetate and dried over Na₂SO₄. The solvent was removed using a rotary evaporator. The Yellow liquid product was obtained with 74 % yield.

Scheme 3: Synthesis of (E)-1-phenyl-3-(*o*-tolyl) prop-2-en-1-one

2.4.4 Synthesis of (E)-1-phenyl-3-(*m*-tolyl) prop-2-en-1-one:

A solution of KOH (1 g) in 10 mL distilled water was added dropwise to the stirring solution of acetophenone (1 mmol, 117 μ L) and *m*-tolualdehyde (1 mmol, 118 μ L) in ethanol (10 mL) in ice bath for 6 hours. The reaction mixture was extracted using ethyl acetate and dried over Na₂SO₄. The solvent was removed using a rotary evaporator. Yellow liquid product was obtained with 95 % yield.

Scheme 4: Synthesis of (E)-1-phenyl-3-(*m*-tolyl) prop-2-en-1-one

2.4.5 Synthesis of (E)-1-phenyl-3-(p-tolyl) prop-2-en-1-one:

A solution of KOH (1 g) in 10 mL distilled water was added dropwise to the stirring solution of acetophenone (1 mmol, 117 μ L) and *p*-tolualdehyde (1 mmol, 118 μ L) in ethanol (10 mL) in ice bath for 6 hours. The reaction mixture was extracted using ethyl acetate and dried over Na₂SO₄. The solvent was removed using a rotary evaporator. White solid product was obtained with 97 % yield.

Scheme 5: Synthesis of (E)-1-phenyl-3-(*p*-tolyl) prop-2-en-1-one

2.4.6 Synthesis of (E)-4-phenylbut-3-en-2-one:

Benzaldehyde (1 mmol, $102 \mu l$) was added dropwise into a solution of NaOH (2.5 mmol, 100 mg) in aqueous ethanol (1:1). After additional stirring for 10 minutes, acetone (1 mmol, $73 \mu L$) was added dropwise and stirred for 1 hour. Water (1 mL) was added to the reaction mixture, which was then filtered. The product was washed with water and purified by re-crystallizing from ethanol and allowed to dry. A yellow-colored crystal was obtained.

Scheme 6: Synthesis of (E)-4-phenylbut-3-en-2-one

2.4.7 Synthesis of (1E,4E)-1,5-diphenylpenta-1,4-dien-3-one:

Benzaldehyde (2 mmol, 204 μ l) was added dropwise into a solution of NaOH (2.5 mmol, 100 mg) in aqueous ethanol (1:1). After additional stirring for 10 minutes, acetone (1 mmol, 73 μ L) was added dropwise and stirred for 1 hour. Water (1 mL) was added to the reaction mixture, which was then filtered. The product was washed with water and purified by re-crystallizing from ethanol and allowed to dry. A yellow-colored crystal was obtained.

Scheme 7: Synthesis of (1E,4E)-1,5-diphenylpenta-1,4-dien-3-one

2.4.8 Synthesis of (1E,4E)-1,5-di-*p*-tolylpenta-1,4-dien-3-one:

p-tolualdehyde (2 mmol, 236 μ L) was added dropwise into a solution of NaOH (2.5 mmol, 100 mg) in aqueous ethanol (1:1). After additional stirring for 10 minutes, acetone (1 mmol, 73 μ L) was added dropwise and stirred for 1 hour. Water (1 mL) was added to the reaction mixture which was then filtered. The product was washed with water and purified by re-crystallizing from ethanol and allowed to dry. Yellow color product was obtained.

Scheme 8: Synthesis of (1E,4E)-1,5-di-*p*-tolylpenta-1,4-dien-3-one

2.5 Catalytic hydrogenation reactions:

2.5.1 Hydrogenation of (E)-1-phenyl-3-(*p*-tolyl) prop-2-en-1-one:

(E)-1-phenyl-3-(p-tolyl) prop-2-en-1-one (1 mmol, 222 mg) was added to the high-pressure reactor (250 mL) along with Ru nanoparticles (0.04 mmol) dispersed in 10 mL distilled water, and the reaction was carried out in the presence of H₂ under stirring at room temperature. After the reaction, the reaction mixture was centrifuged at 7000 rpm for 3 minutes. The product was extracted from the water portion using dichloromethane (10 mL), and the combined organic layer was dried over anhydrous Na₂SO₄, and all the volatiles were removed using a rotary evaporator.

2.5.2 Hydrogenation of (E)-1-phenyl-3-(o-tolyl) prop-2-en-1-one:

(E)-1-phenyl-3-(o-tolyl) prop-2-en-1-one (1mmol, 222 mg) was added to the high-pressure reactor (250 mL) along with Ru nanoparticles (0.04 mmol) dispersed in 10 mL distilled water and the reaction was carried out in the presence of H₂ (4 bar) under stirring at room temperature for 12 hours. After the reaction, the reaction mixture was centrifuged at 7000 rpm for 3 minutes. Product was extracted from water portion using dichloromethane (10 mL), and the combined organic layer was dried over anhydrous Na₂SO₄, and all the volatiles were removed using a rotary evaporator.

2.5.3 Hydrogenation of chalcone:

Chalcone (1 mmol, 208 mg), along with Ru nanoparticles (0.04 mmol) dispersed in 10 mL distilled water in the presence of H₂ under stirring at room temperature, was performed in both a high-pressure reactor (250 mL) and a round-bottom flask (50 mL). After the reaction, the reaction mixture was centrifuged at 7000 rpm for 3 minutes. Product was extracted from water portion using dichloromethane (10 mL), and the combined organic layer was dried over anhydrous Na₂SO₄, and all the volatiles were removed using a rotary evaporator.

Chapter 3: Results and discussion:

3.1 Characterization of the Ru nanoparticles:

Ru nanoparticles were characterized by P-XRD. Powder X-ray diffractogram of Ru nanoparticles shows 20 value at 43°, which corresponds to (101) plane of hexagonal closed-packed Ru nanoparticles. P-XRD spectrum showing the broad peaks indicating the amorphous nature and small size of Ru. To know about the morphology of the catalyst, FE-SEM analysis was carried out. FE-SEM image and corresponding EDX spectra confirmed the presence of Ru.

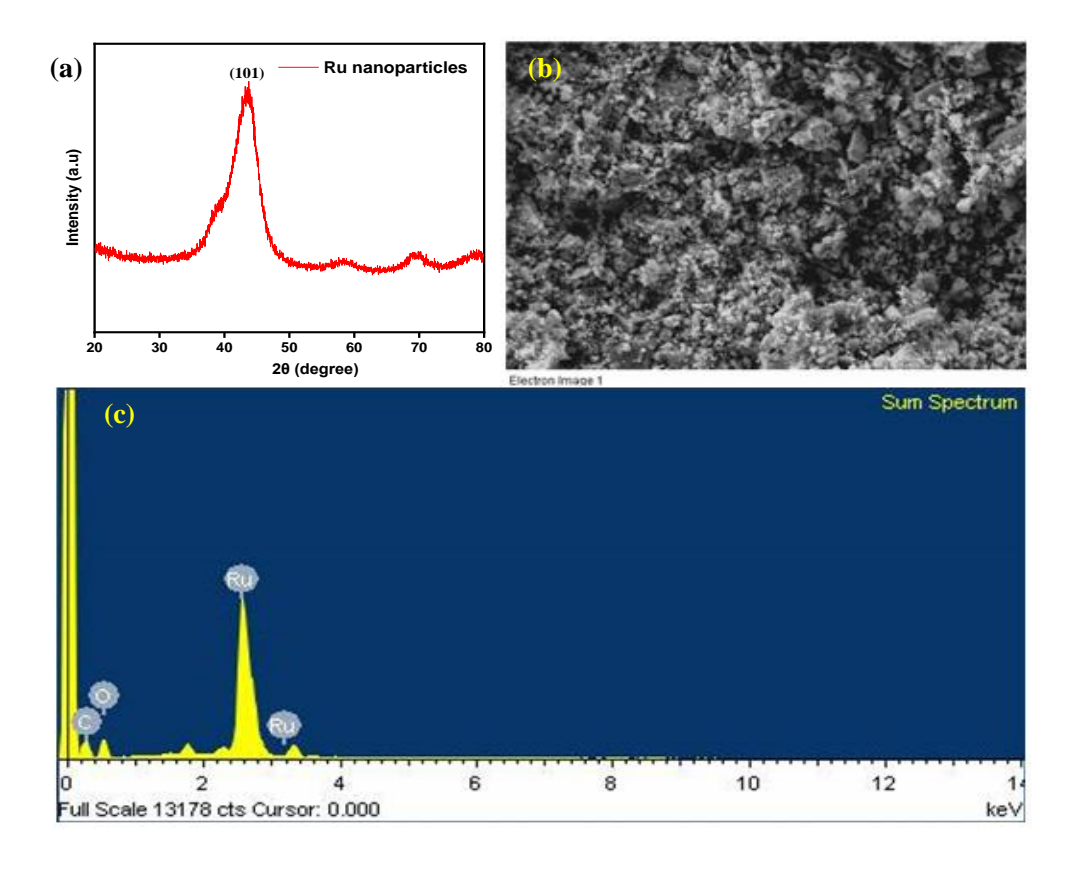


Figure 1: (a) P-XRD pattern, (b) FE-SEM image, and corresponding (c) EDX Spectra of Ru nanoparticles.

3.2 Characterization of lignin:

Lignin was characterized by FTIR spectroscopy. FTIR spectra of lignin, in this spectrum, peaks at 3429 cm⁻¹ and 2945 cm⁻¹ show OH and C-H stretching,

respectively. Peaks in 1709 and 1625 cm⁻¹ are assigned to carbonyl C=O. Peaks at 1520 and 1426 cm⁻¹ are showing aromatic rings. The peak at 1365 cm⁻¹ is attributed to C=O stretching of the syringyl units, and peaks at 1210 cm⁻¹ correspond to C-C, C-O, and C=O stretching of the guaiacyl units. Both 1114 and 1035 cm⁻¹ peaks are attributed to ether C-O bonds. Peaks at 830 cm⁻¹ show aromatic C-H out of plane bending. Besides these, there are bands observed at 570 and 465 cm⁻¹.

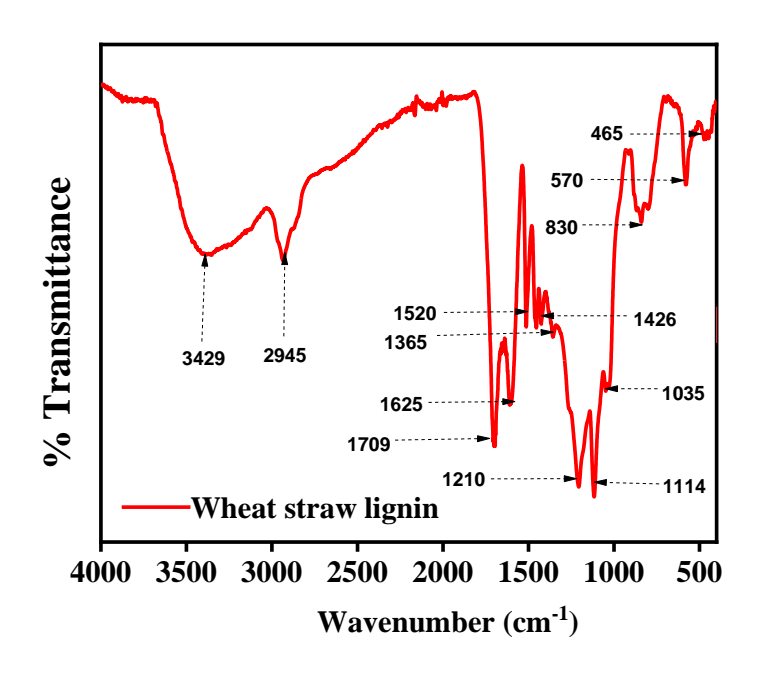


Figure 2: FTIR Spectra of wheat straw lignin.

3.3 Characterization of 2,6-dibenzylcyclohexan-1-one:

¹H NMR (CDCl₃, 400 MHz): δ (ppm) 7.74 (s, 2H), 7.41-7.39 (d, 4H), 7.36-7.32 (t, 4H), 7.29-7.25 (t, 2H), 2.88-2.85 (t, 4H), 1.76-1.69 (m, 2H). ¹³C NMR (CDCl₃, 100 MHz): δ (ppm) 190.37, 136.91, 136.18, 135.96, 130.34, 128.56, 128.36, 28.43, 23.00. LCMS: Calculated 275.1430 m/z, Observed 275.1452 m/z.

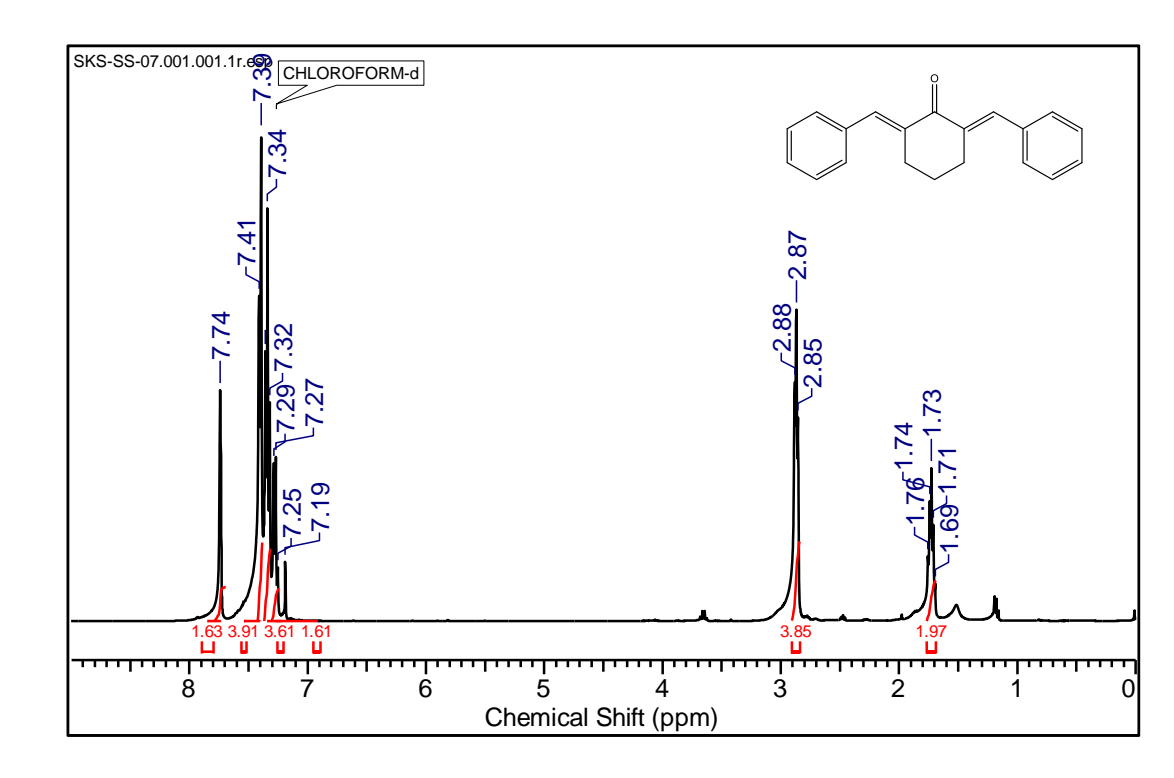


Figure 3: ¹H spectra of 2,6-dibenzylcyclohexan-1-one.

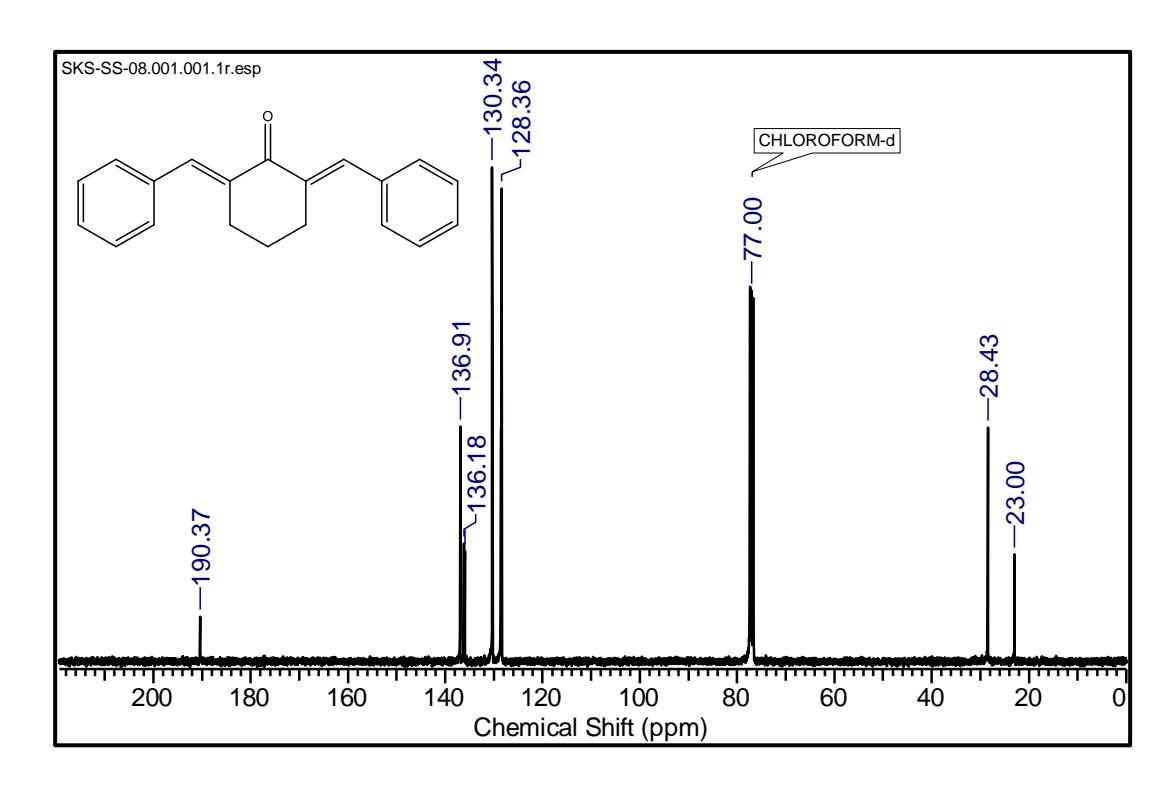


Figure 4: ¹³C spectra of 2,6-dibenzylcyclohexan-1-one.

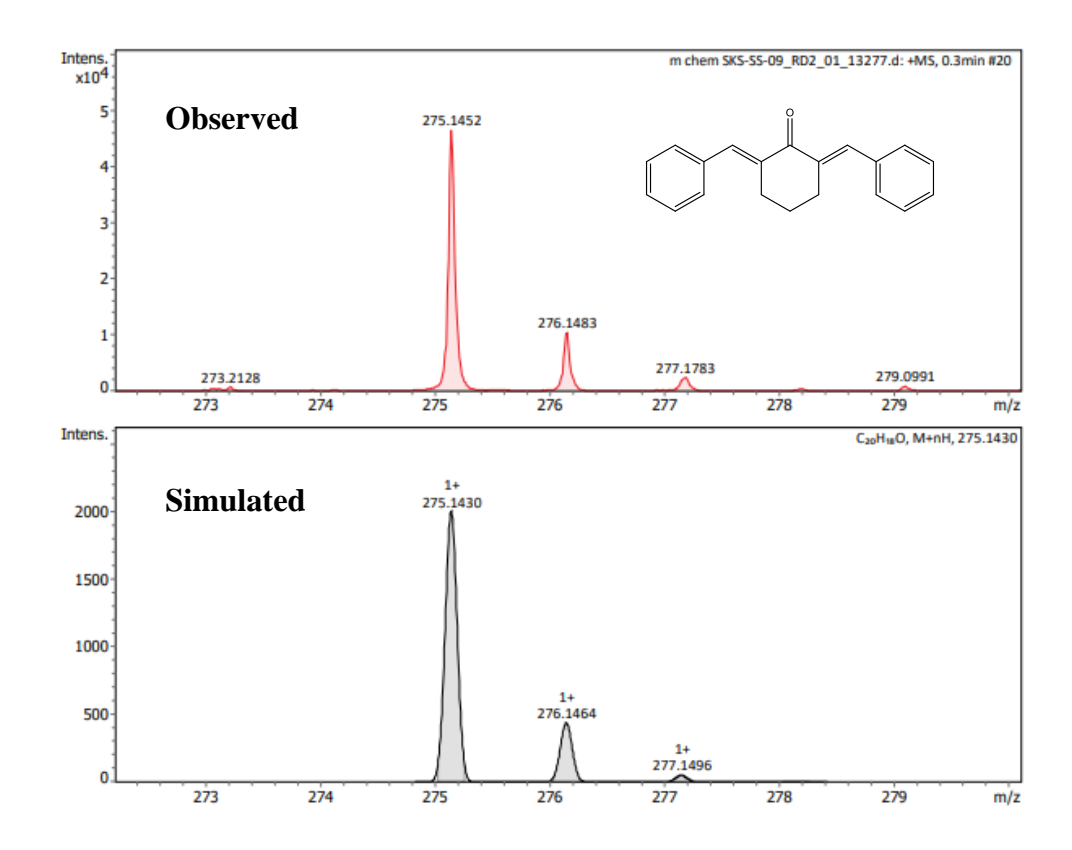


Figure 5: LCMS Spectra of 2,6-dibenzylcyclohexan-1-one.

3.4 Characterization of chalcone:

 1 H NMR (CDCl₃, 400 MHz): δ (ppm) 8.04-8.03 (m, 2H), 7.84-7.81 (d, 1H), 7.67-7.42 (m, 9H). 13 C NMR (CDCl₃, 100 MHz): δ (ppm) 190.59, 144.87, 138.22, 134.89, 132.79, 130.54, 128.97, 128.63, 128.51, 128.45, 122.11.

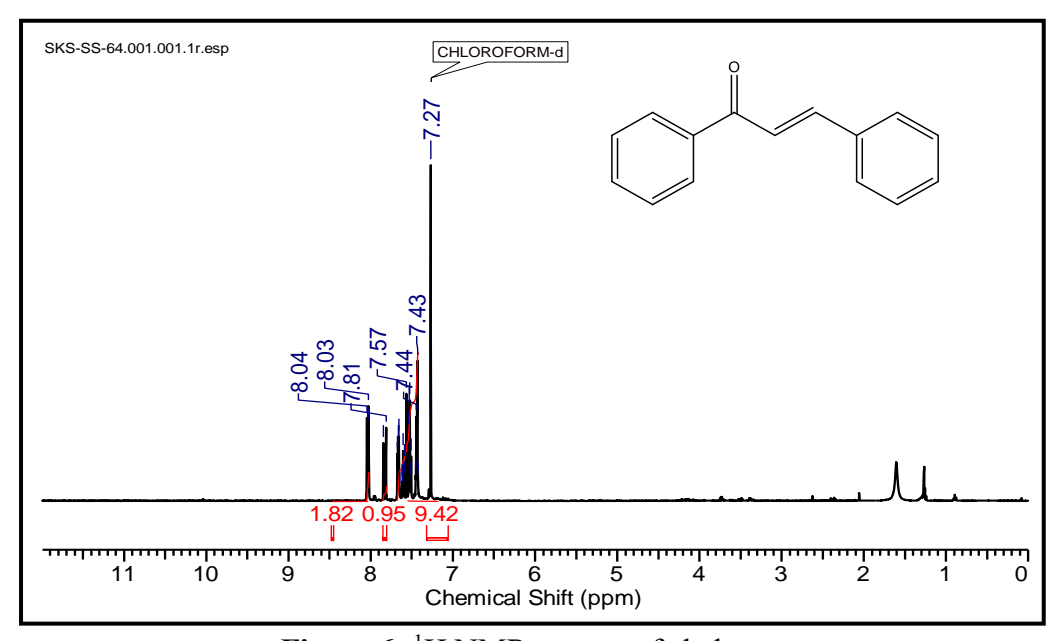


Figure 6: ¹H NMR spectra of chalcone.

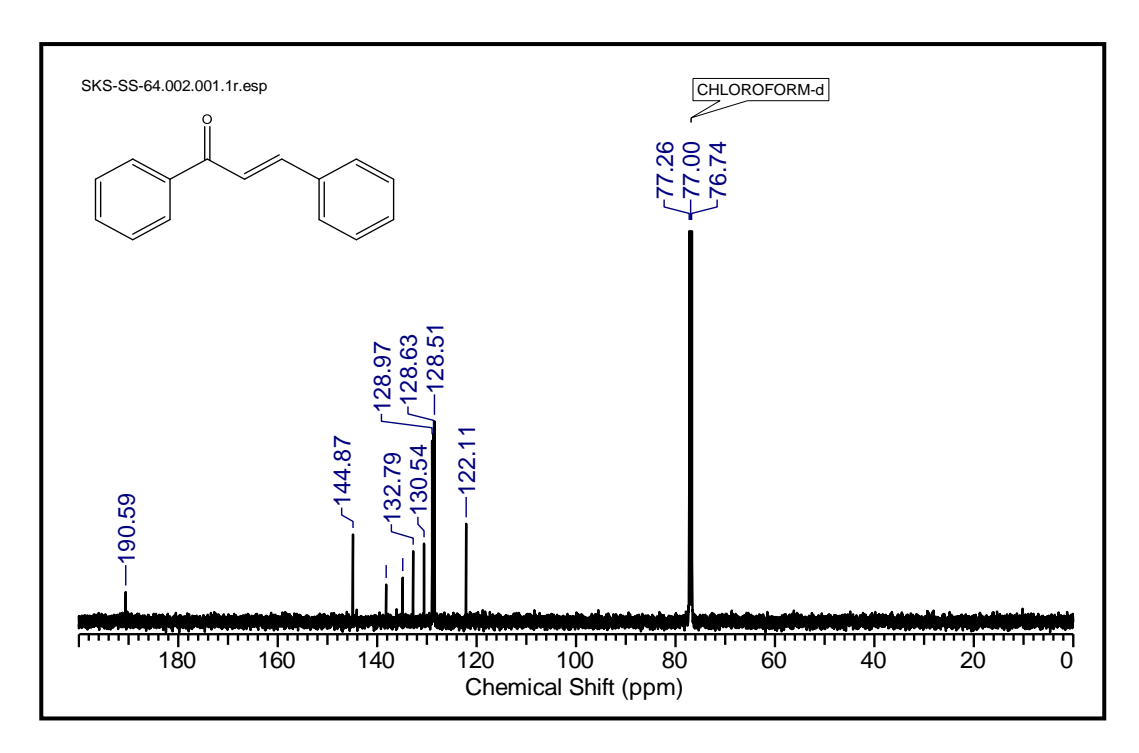


Figure 7: ¹³C NMR spectra of chalcone.

3.5 Characterization of (E)-1-phenyl-3-(*o*-tolyl) prop-2-en-1-one:

¹H NMR (CDCl₃, 400 MHz): δ (ppm) 8.18-8.15 (d, 1H), 8.08-8.07 (m, 2H), 7.75-7.28 (m, 8H), 2.52 (s, 3H). ¹³C NMR (CDCl₃, 100 MHz): δ (ppm) 190.47, 142.45, 138.36, 138.23, 133.91, 132.77, 130.91, 130.25, 128.61, 128.50, 126.40, 126.33, 123.12, 19.86.

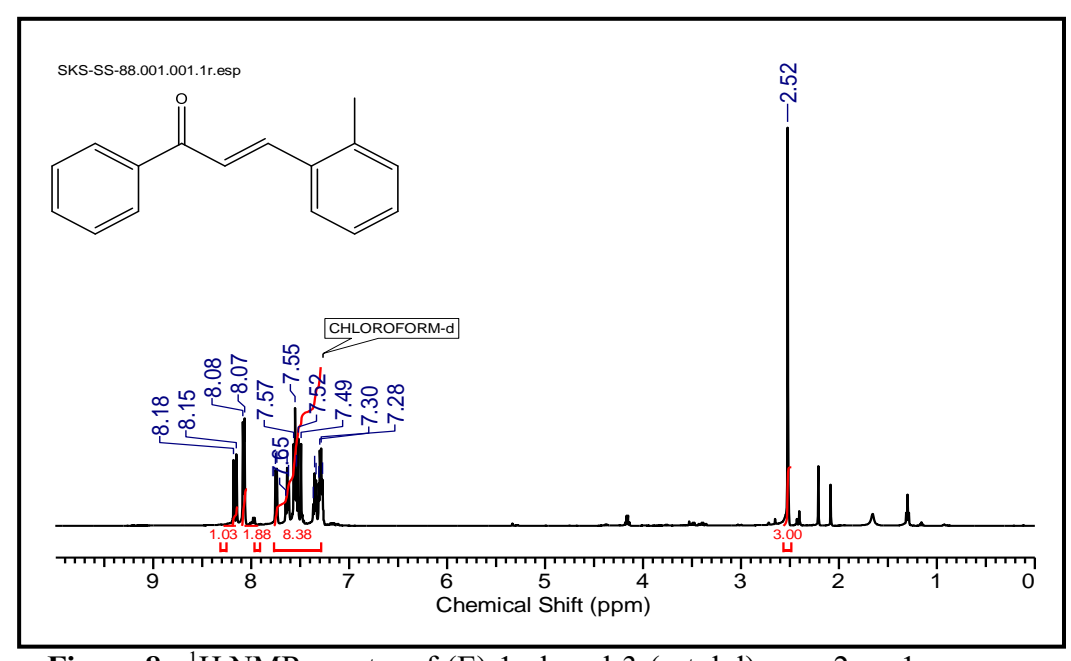


Figure 8: ¹H NMR spectra of (E)-1-phenyl-3-(*o*-tolyl) prop-2-en-1-one.

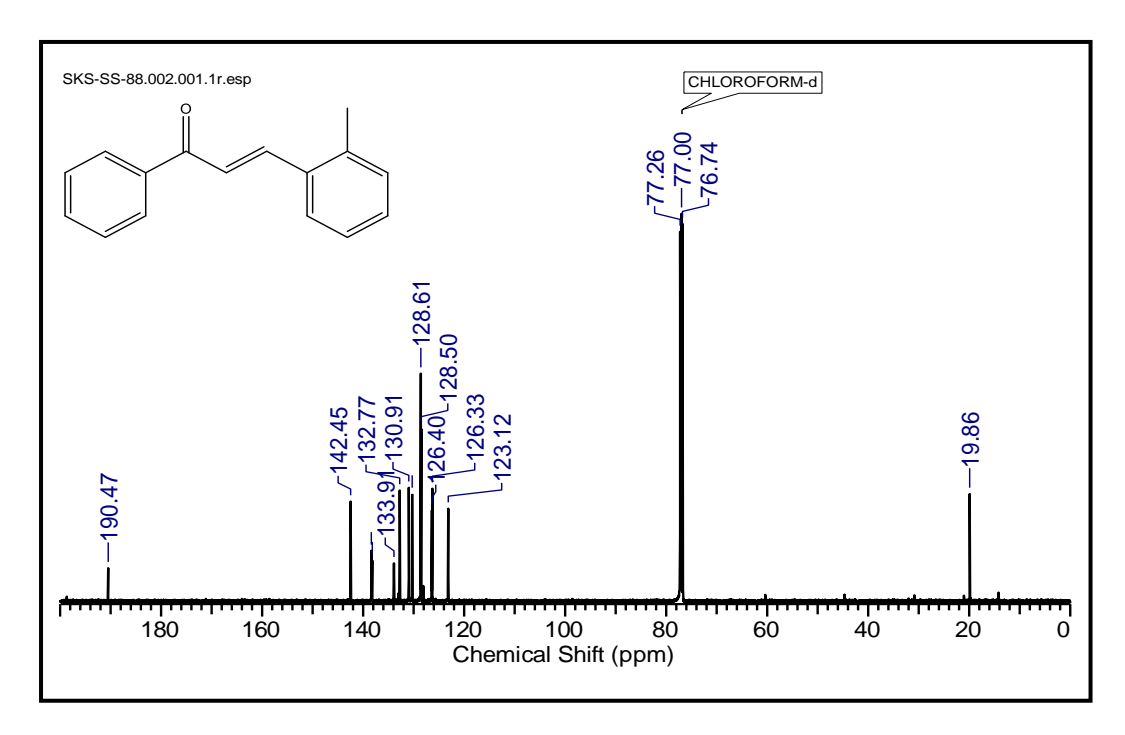


Figure 9: ¹³C NMR spectra of (E)-1-phenyl-3-(o-tolyl) prop-2-en-1-one.

3.6 Characterization of (E)-1-phenyl-3-(*m*-tolyl) prop-2-en-1-one:

¹H NMR (CDCl₃, 400 MHz): δ (ppm) 8.09-8.0 (m, 2H), 8.87-8.83 (d, 1H), 7.65-7.29 (m, 8H), 2.45 (s, 3H). ¹³C NMR (CDCl₃, 100 MHz): δ (ppm) 190.67, 144.94, 141.08, 138.35, 132.65, 132.14, 129.70, 128.57, 128.47, 128.45, 121.10, 21.53.

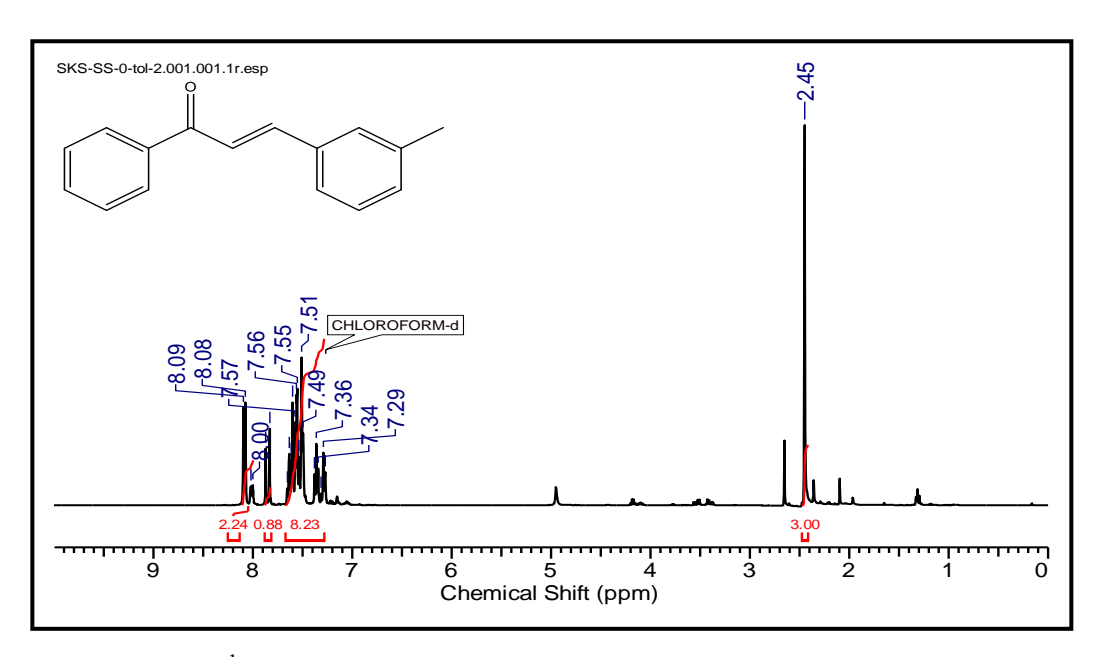


Figure 10: ¹H NMR spectra of (E)-1-phenyl-3-(*m*-tolyl) prop-2-en-1-one.

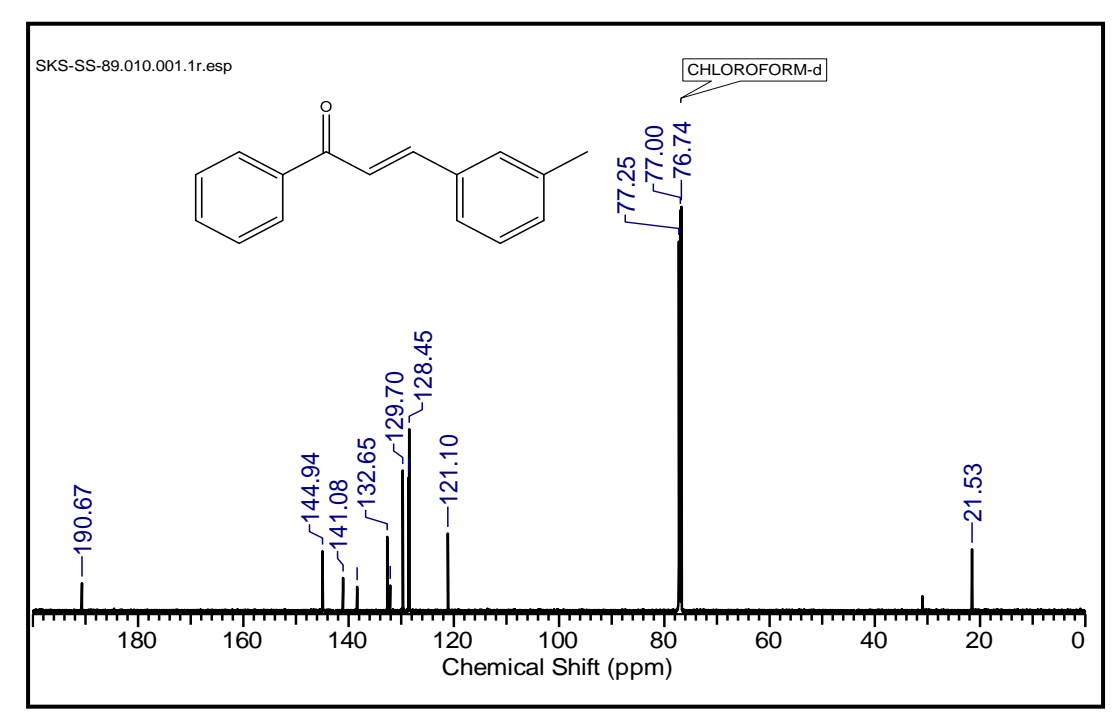


Figure 11: ¹³C NMR spectra of (E)-1-phenyl-3-(*m*-tolyl) prop-2-en-1-one.

3.7 Characterization of (E)-1-phenyl-3-(p-tolyl) prop-2-en-1-one:

¹H NMR (CDCl₃, 400 MHz): δ (ppm) 8.07-8.06 (m, 2H), 8.86-8.83 (d, 1H), 7.65-7.29 (m, 8H), 2.44 (s, 3H). ¹³C NMR (CDCl₃, 100 MHz): δ (ppm) 190.67, 144.94, 141.08, 138.35, 132.65, 132.14, 129.70, 128.57, 128.47, 128.45, 126.40, 121.10, 21.53.

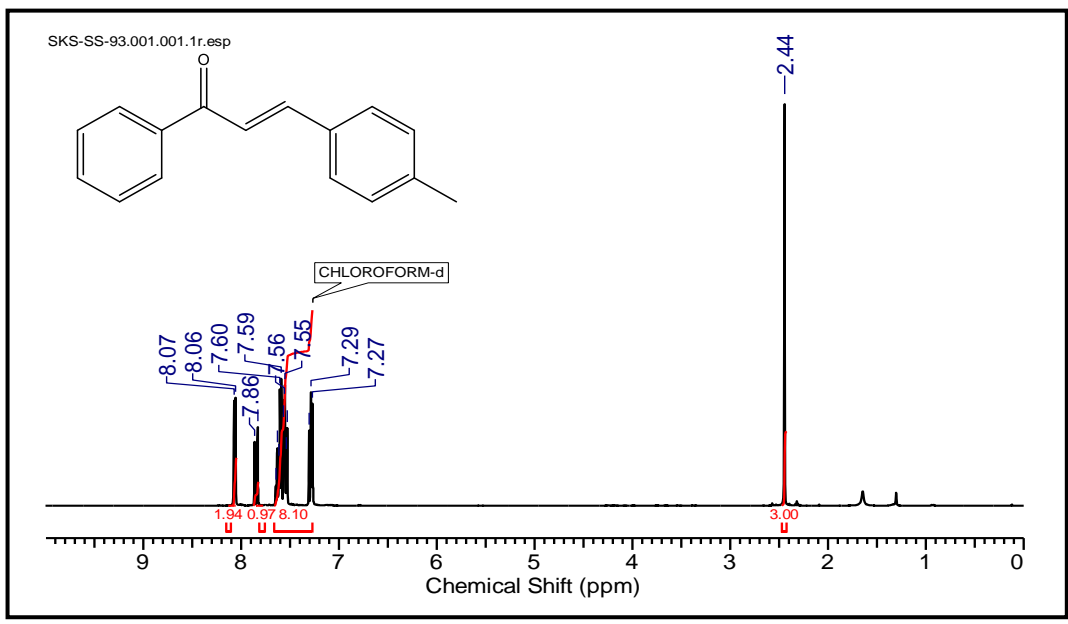


Figure 12: ¹H NMR spectra of (E)-1-phenyl-3-(*p*-tolyl) prop-2-en-1-one.

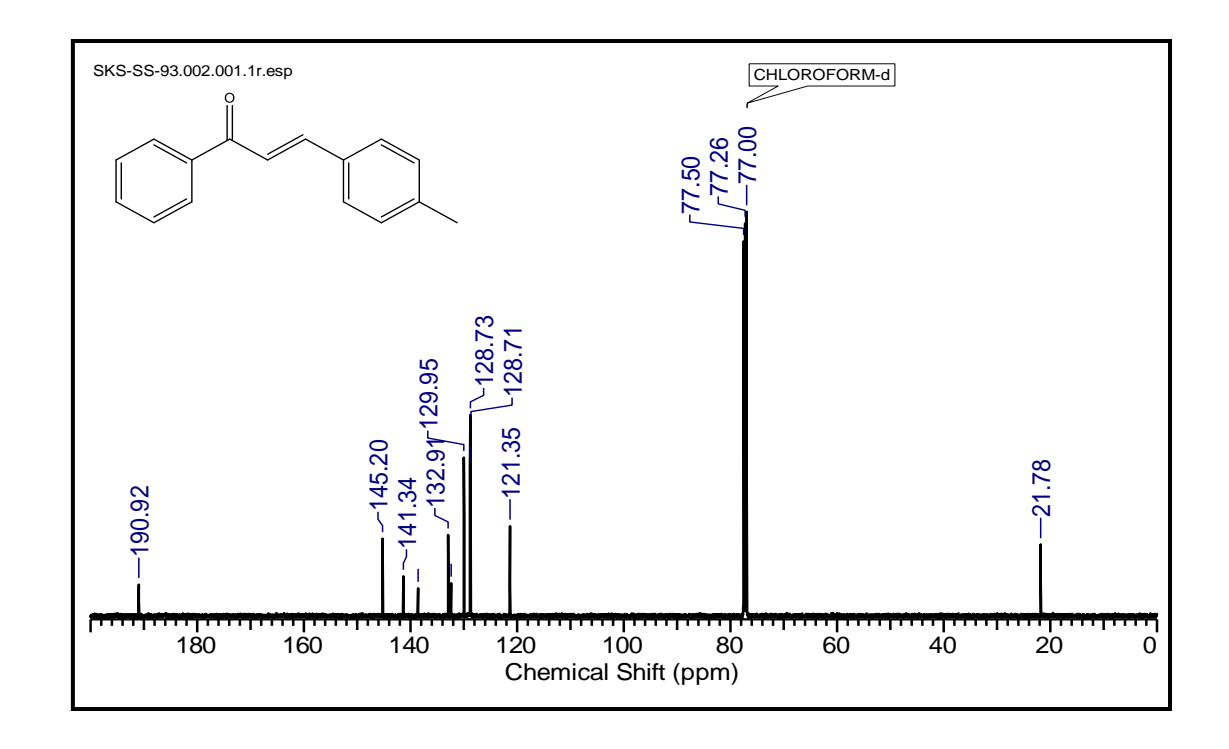


Figure 13: ¹³C NMR spectra of (E)-1-phenyl-3-(*p*-tolyl) prop-2-en-1-one.

3.8 Characterization of (E)-4-phenylbut-3-en-2-one:

 1 H NMR (CDCl₃, 400 MHz): δ (ppm) 7.78-7.74 (d, 1H), 7.65-7.63 (m, 2H), 7.44-7.42 (m, 3H), 7.12-7.08 (d, 1H), 1.56 (s, 3H). 13 C NMR (CDCl₃, 100 MHz): δ (ppm) 206.73, 143.08, 134.53, 130.25, 128.70, 128.13, 125.15, 30.66.

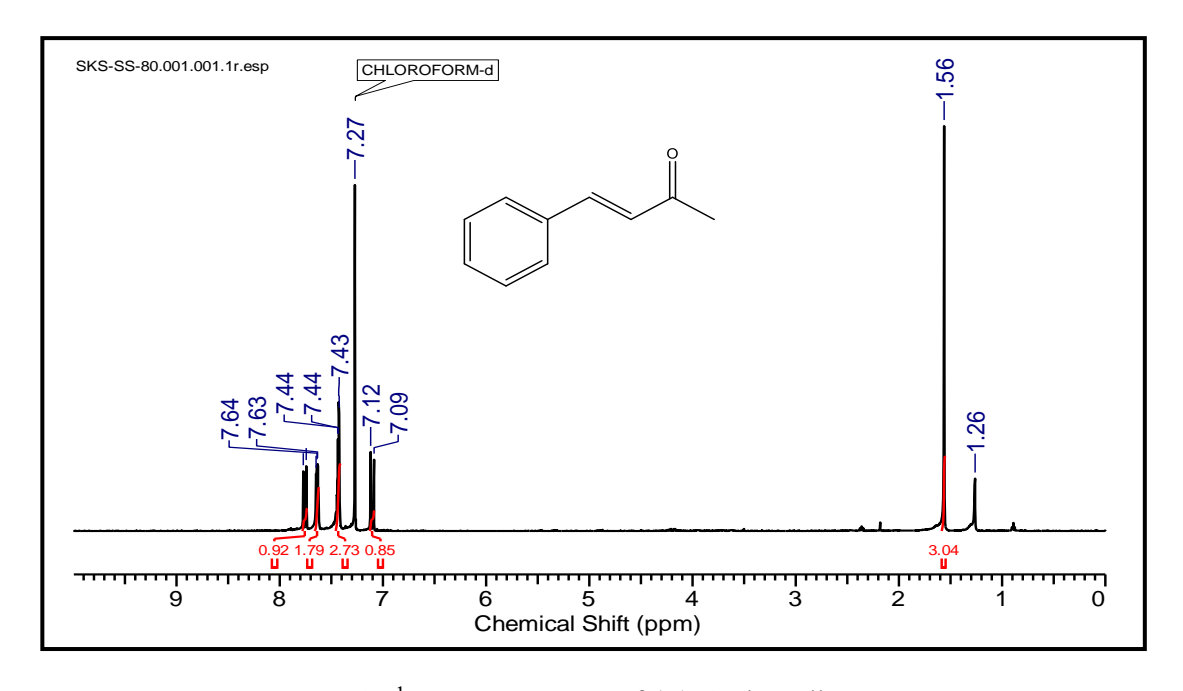


Figure 14: ¹H NMR spectra of (E)-4-phenylbut-3-en-2-one.

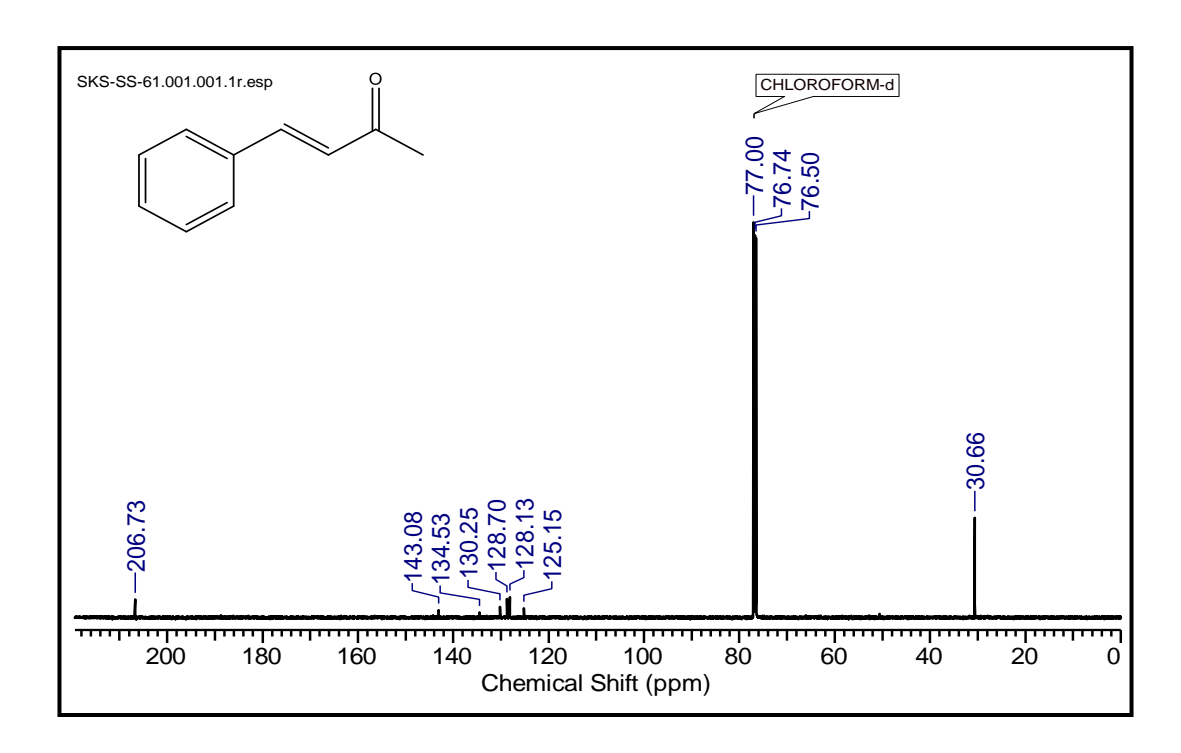


Figure 15: ¹³C NMR spectra of (E)-4-phenylbut-3-en-2-one.

3.9 Characterization of (1E,4E)-1,5-diphenylpenta-1,4-dien-3-one:

 1 H NMR (CDCl₃, 400 MHz): δ (ppm) 7.78-7.74 (d, 2H), 7.64-7.63 (m, 4H), 7.44-7.43 (m, 6H), 7.12-7.08 (d, 2H). 13 C NMR (CDCl₃, 100 MHz): δ (ppm) 188.93, 143.32, 134.18, 130.50, 128.96, 128.39, 125.42.

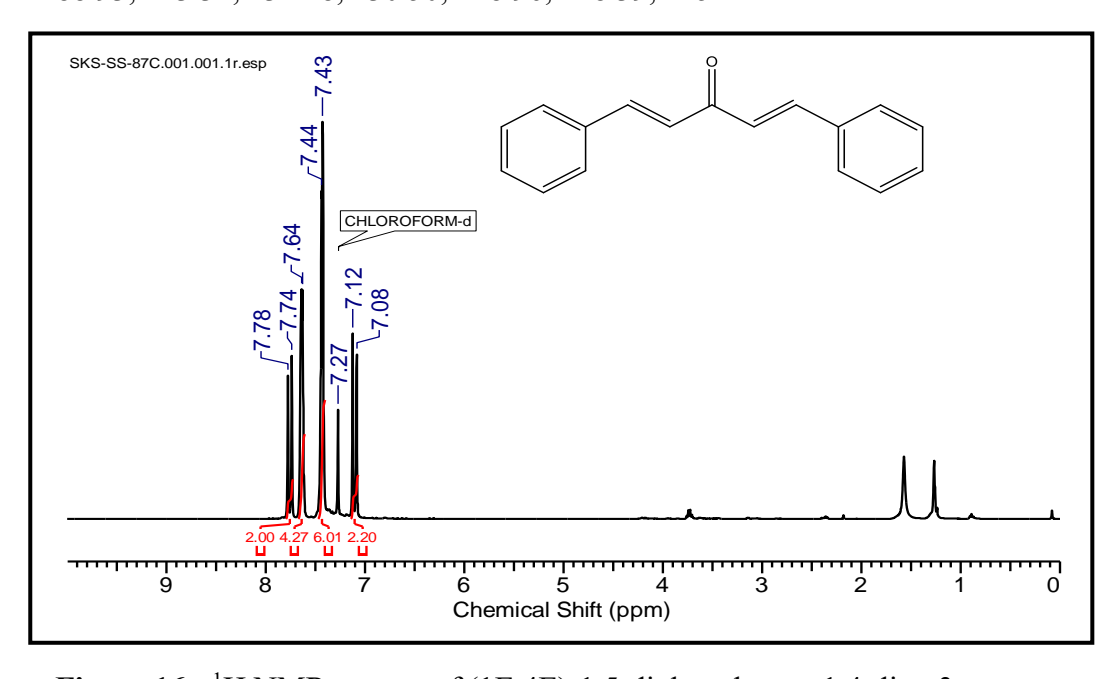


Figure 16: ¹H NMR spectra of (1E,4E)-1,5-diphenylpenta-1,4-dien-3-one.

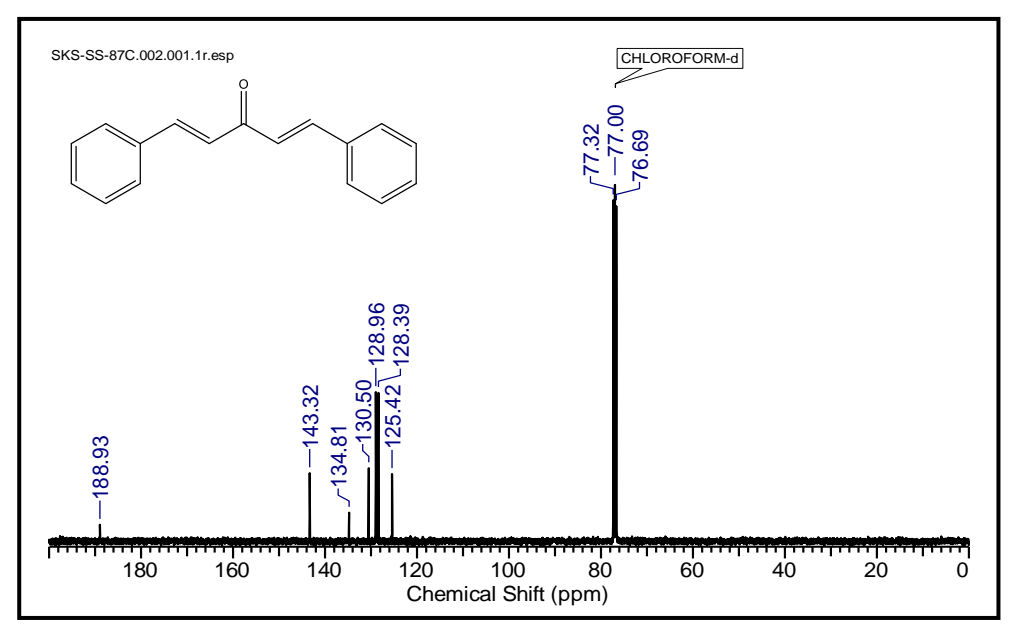


Figure 17: ¹³C NMR spectra of (1E,4E)-1,5-diphenylpenta-1,4-dien-3-one.

3.10 Characterization of (1E,4E)-1,5-di-*p*-tolylpenta-1,4-dien-3-one:

 1 H NMR (CDCl₃, 400 MHz): δ (ppm) 7.79-7.75 (d, 2H), 7.58-7.57 (m, 4H), 7.32-7.29 (m, 6H), 7.12-7.08 (d, 2H). 13 C NMR (CDCl₃, 100 MHz): δ (ppm) 188.81, 142.90, 140.70, 131.86, 129.44, 128.13, 124.33, 21.26.

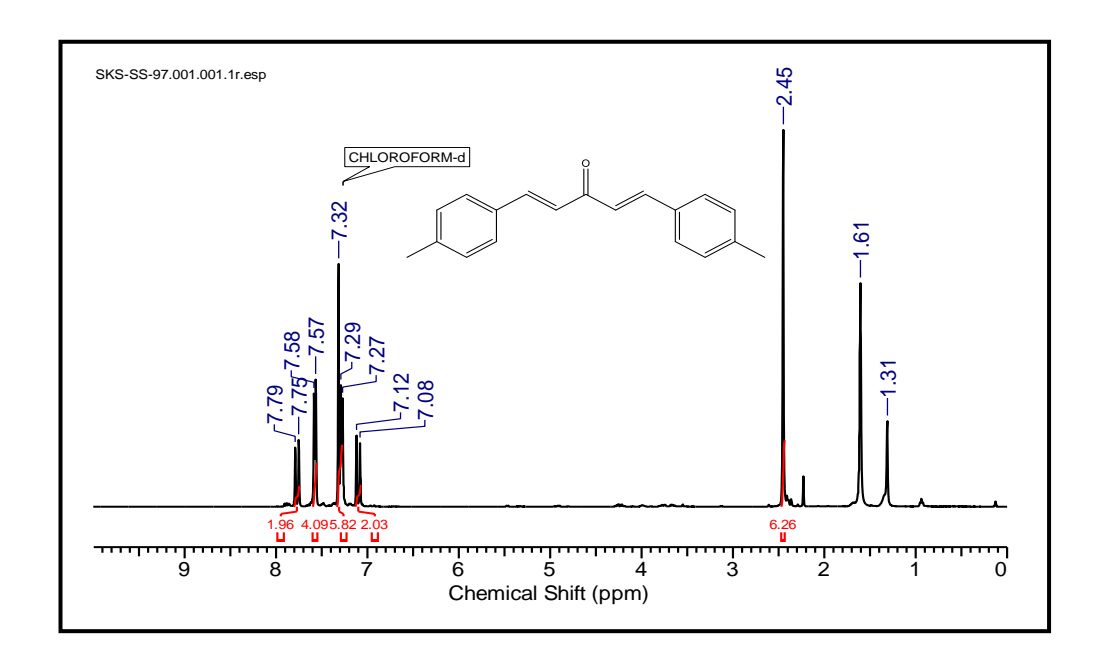


Figure 18: ¹H NMR spectra of (1E,4E)-1,5-di-*p*-tolylpenta-1,4-dien-3-one.

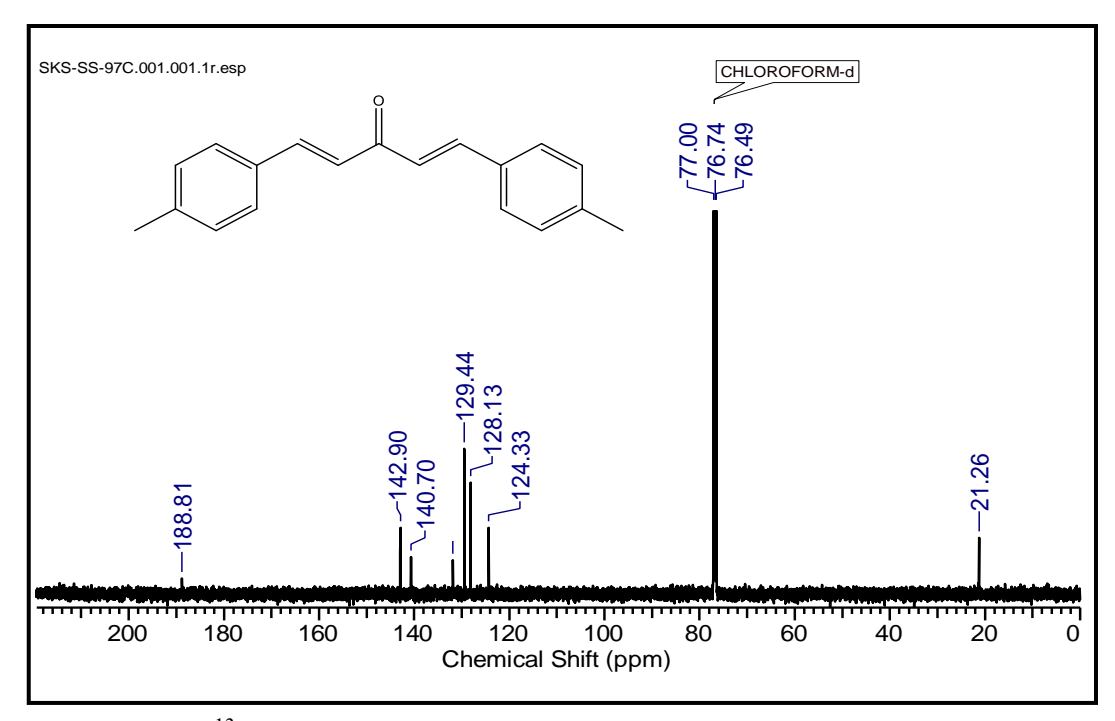


Figure 19: ¹³C NMR spectra of (1E,4E)-1,5-di-*p*-tolylpenta-1,4-dien-3-one.

3.11 Hydrogenation reaction of (E)-1-phenyl-3-(*p*-tolyl) prop-2-en-1-one:

The catalytic hydrogenation of (E)-1-phenyl-3-(p-tolyl) prop-2-en-1-one in water using Ru catalyst was performed at room temperature under 4 bar of H₂ for 8 h. This reaction achieved 81% conversion with product selectivities spread across four compounds (a-d), the highest being product a with 28% selectivity and 66% yield (Table 1, entry 1). Further, when the reaction time was extended for 12 h, >99% conversion with exclusive selectivity (>99%) and yield (95%) for product b was achieved, indicating highly selective hydrogenation towards a single product under prolonged reaction time with high efficiency (Table 1 entry 2).

Scheme 9: Hydrogenation of (E)-1-phenyl-3-(*p*-tolyl) prop-2-en-1-one

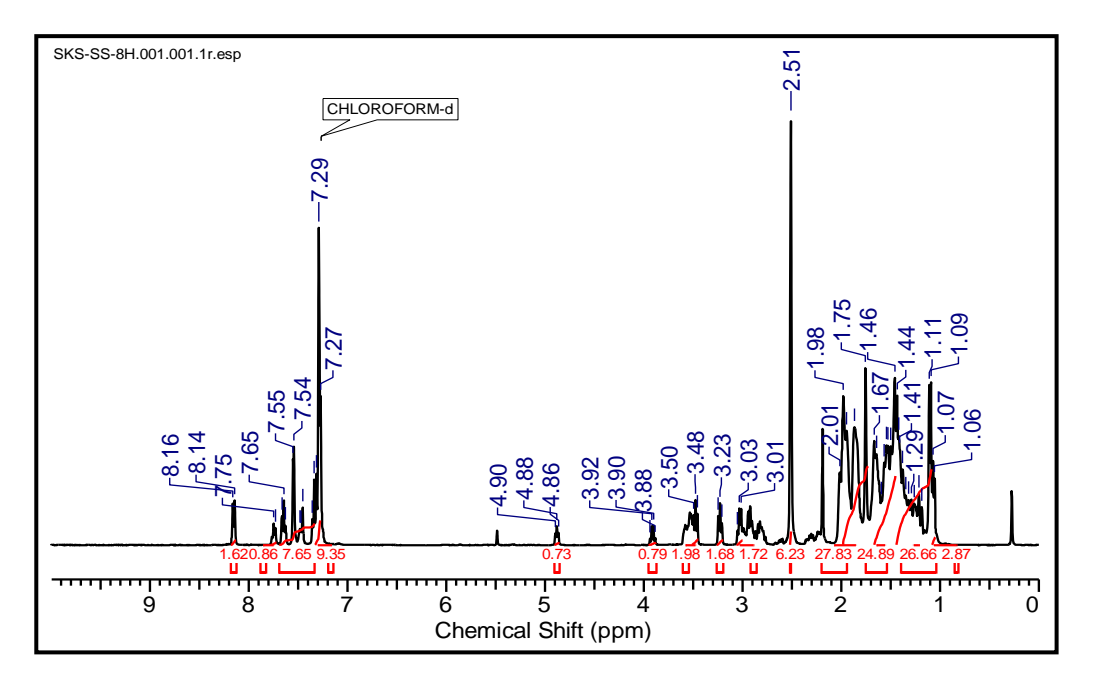


Figure 20: ¹H NMR spectra of hydrogenation of (E)-1-phenyl-3-(*p*-tolyl) prop-2-en-1-one for 8 h.

Scheme 10: Hydrogenation of (E)-1-phenyl-3-(*p*-tolyl) prop-2-en-1-one for 12 h.

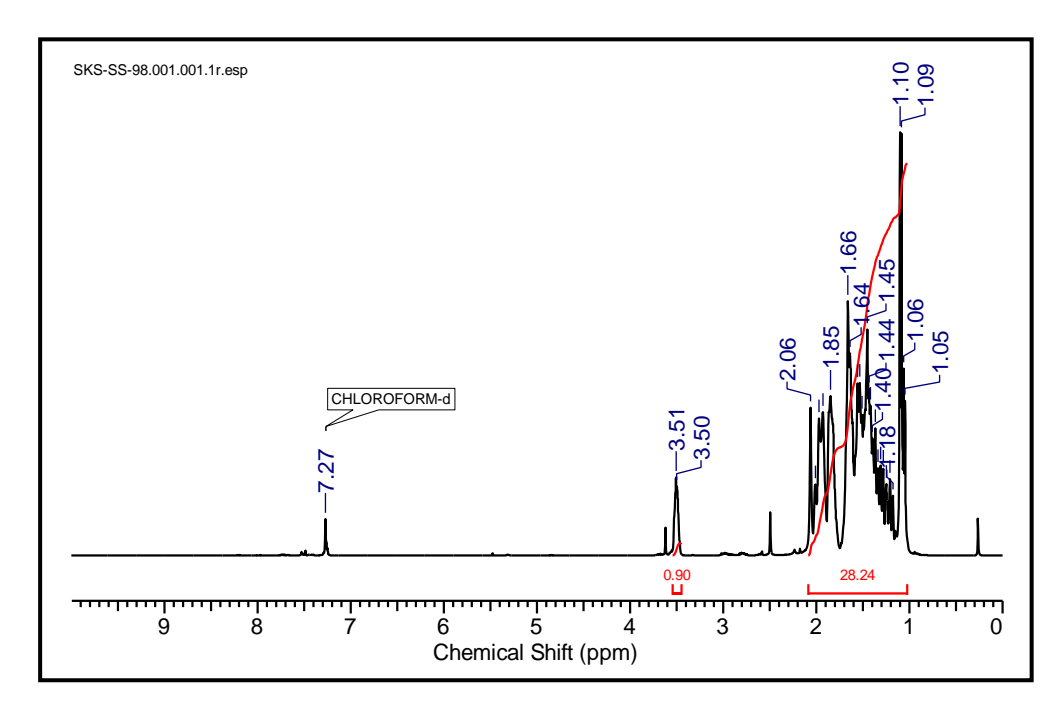


Figure 21: ¹H NMR spectra of hydrogenation of (E)-1-phenyl-3-(*p*-tolyl) prop-2-en-1-one for 12 h.

Table 2: Optimization table for hydrogenation of (E)-1-phenyl-3-(p-tolyl) prop-2-en-1-one

Entry	Substrate	Time	Conversion (%)	Selectivity (%)				Yield (%)			
				a	b	c	d	a	b	c	d
1.		8 h	81	19	23	16	22	66	12	3	34
2.		12 h	> 99	-	> 99	-	-	-	95 ⁱ	-	-
Reaction conditions: Ru nanoparticles (0.04 mmol), substrate (1 mmol), water (10 mL), H ₂ (4 bar), room temperature, t h. i=isolated yield.											
	100 -		Conversion Reactant Selectivity of a Selectivity of b Selectivity of c								
	80 -		Selectivity of d								

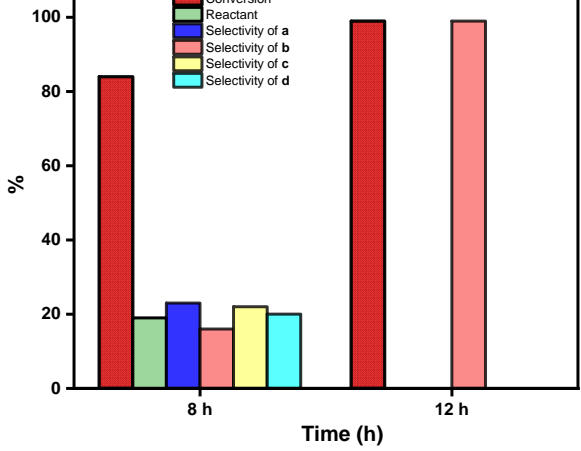


Figure 22: Selectivity and conversion for hydrogenation of (E)-1-phenyl-3-(*p*-tolyl) prop-2-en-1-one in different time scales.

In experiments conducted at different time intervals to investigate their impact on the hydrogenation of (E)-1-phenyl-3-(*p*-tolyl) prop-2-en-1-one, we noted varying conversion rates: 81% at 8 hours and >99% at 12 hours. Additionally, the selectivity for the desired hydrogenated product, 1-cyclohexyl-3-(4-methylcyclohexyl) propan-1-ol (**b**), increased significantly as the reaction duration extended, with selectivity rising from 23% to >99%.

3.12 Hydrogenation reaction of (E)-1-phenyl-3-(o-tolyl) prop-2-en-1-one:

The catalytic hydrogenation of (E)-1-phenyl-3-(*o*-tolyl) prop-2-en-1-one in water using Ru nanoparticles was performed at room temperature under 4 bar of H₂ for 12 h. This reaction achieved 61 % conversion with product selectivities spread across two compounds (a-b). The Selectivity and yield of the products a and b are 45%, 55% and 14% and 6% respectively.

Scheme 11: Hydrogenation of (E)-1-phenyl-3-(o-tolyl) prop-2-en-1-one

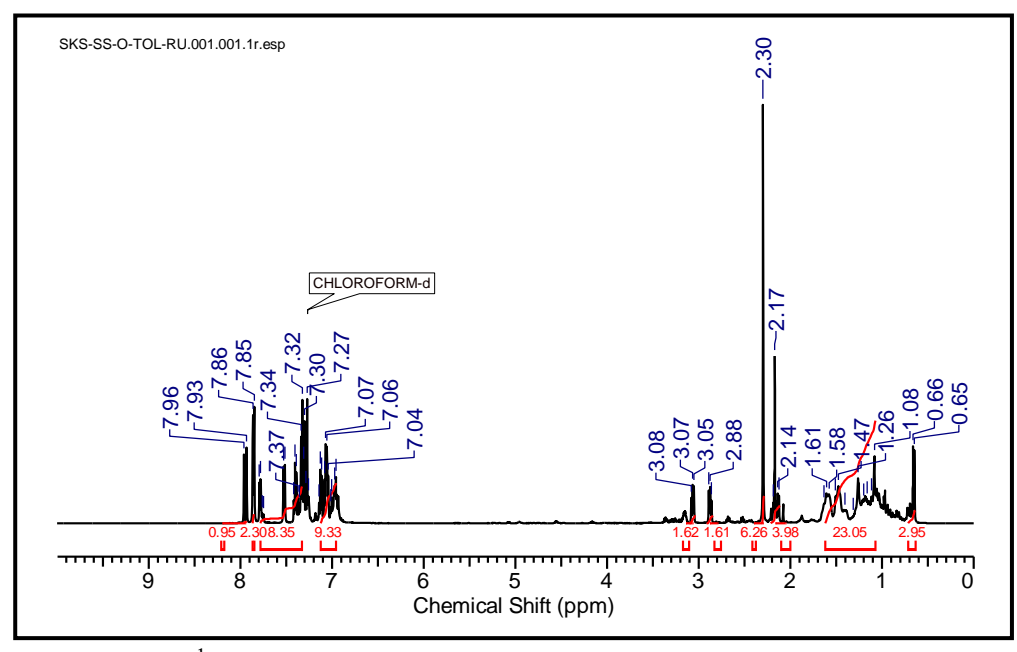


Figure 23: ¹H NMR spectra of hydrogenation of (E)-1-phenyl-3-(*o*-tolyl) prop-2-en-1-one.

3.13 Hydrogenation reaction of chalcone:

The catalytic hydrogenation of chalcone in water using Ru nanoparticles was performed at room temperature using H₂ balloon for 24 h. This reaction achieved 57 % conversion with product a with >99% selectivity and 56 % yield (Table 1, entry 1). Further, increasing the H₂ pressure to 2 bar resulted in 77 % conversion with product selectivities spread across three compounds (a-c), the highest being product a with 37 % selectivity (Table 1, entry 2). Further, when H₂ pressure was extended to 4 bar, >99% conversion with compounds b (52 % selectivity and 56 % yield) and c (48 % selectivity and 30 % yield) indicating highly selective hydrogenation towards fully hydrogenated product under higher H₂ pressure with high efficiency (Table 1 entry 3).

Scheme 12: Hydrogenation of chalcone with 1 bar H₂ pressure.

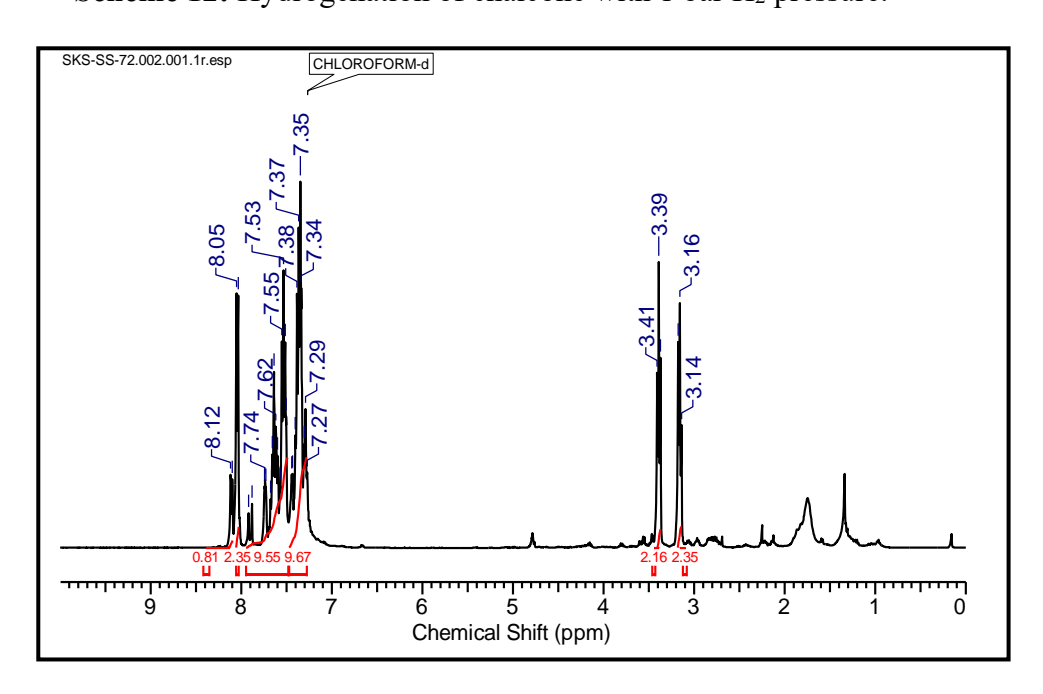
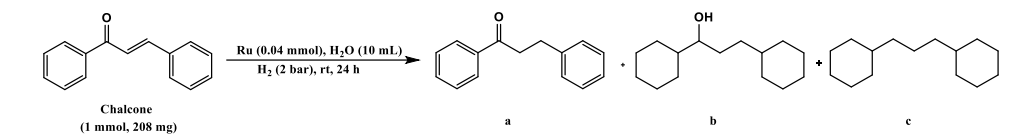


Figure 24: ¹H NMR spectra of the hydrogenation of chalcone with 1 bar H₂ pressure.



Scheme 13: Hydrogenation of chalcone with 2 bar H₂ pressure.

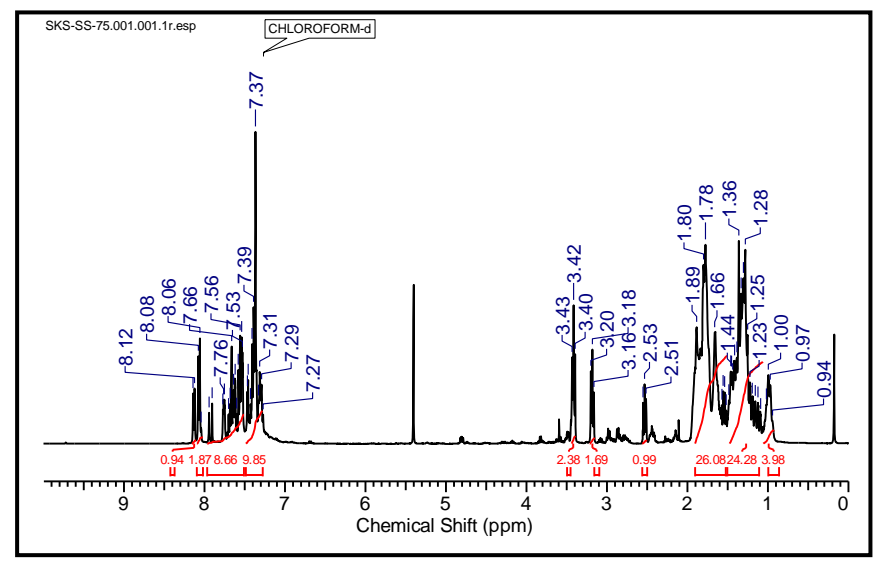


Figure 25: ¹H NMR spectra of hydrogenation of chalcone with 2 bar H₂ pressure.

Scheme 14: Hydrogenation of chalcone with 4 bar H₂ pressure.

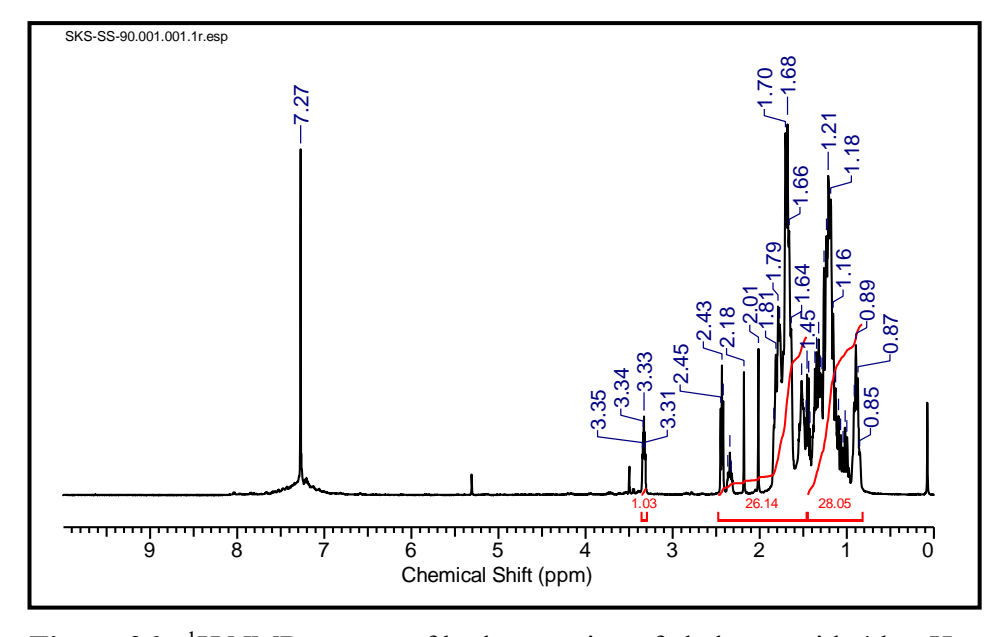


Figure 26: ¹H NMR spectra of hydrogenation of chalcone with 4 bar H₂ pressure.

Table 3: Optimization table for hydrogenation of chalcone

Entry	Substrate	H ₂ (bar)	Conversion (%)	Selectivity (%)			Yield (%)		
				a	b	с	a	b	с
1.		1 bar	57	> 99	-	-	56	-	-
2.	O C	2 bar	77	37	31	32	5	6	9
3.		4 bar	> 99	-	52	48	-	56	30
Reaction o	conditions: Ru catalyst (0.04 mr	nol), substrate (1 mm	bl), water (10 mL), H ₂ (bar), room temp	perature, 24 h.				

Conversion
Reactant
Selectivity of a
Selectivity of c

40

40

40

H₂ Pressure (bar)

Figure 27: Selectivity and conversion for chalcone in different H₂ pressure.

In experiments conducted at different H₂ pressures investigate their impact on the hydrogenation of chalcone, we noted varying conversion rates: 57 % in 1 bar, 77 % in 2 bar, and >99 % in 4 bar H₂ pressure. Additionally, the selectivity for the desired hydrogenated products, 1,3-dicyclohexylpropan-1-ol (**b**) and 1,3-dicyclohexylpropane (**c**), increased significantly as the H₂ pressure increased, with selectivity rising from 31 % to 52 % and 32 % to 48 %, respectively.

Chapter 4

Conclusions and scope of work:

We successfully synthesized ruthenium (Ru) nanoparticles, which were used as catalysts for the hydrogenation of reactions. Ru nanoparticles were characterized using powder X-ray diffraction (P-XRD) analysis. Cellulose and lignin were extracted from wheat straw and characterized by Fourier-transform infrared (FTIR) spectroscopy. These components play a crucial role in the production of fuels and chemicals. Furthermore, we synthesized various high-carbon substrates through aldol condensation reactions between aldehydes and ketones and characterized them using ¹H NMR and ¹³C NMR spectroscopy. Subsequently, we carried out catalytic hydrogenation reactions of these substrates at room temperature, with the products characterized by ¹H NMR spectroscopy.

This project aims to turn agricultural waste like wheat straw, wood dust, and rice straw into useful biofuels. First, we separated the two main parts of the biomass—lignin and cellulose. Lignin breaks down into simpler chemicals such as vanillin and other related compounds, while cellulose breaks down into furan-based chemicals. These compounds can react with ketones to form larger molecules. In the next step, we used catalysts to carry out reactions like hydrogenation and hydrodeoxygenation to turn these molecules into hydrocarbons. These hydrocarbons are being developed to meet the standards for jet fuel. Overall, this work helps create renewable fuels and adds value to farm waste by converting it into energy-rich products.

References:

- 1. H. Yousefi, V. Azari, A. Khazaeian, *Ind. Crops Prod.* 2018, 115, 26-31.
- **2.** S. Wu, D. Shen, J. Hu, H. Zhang, R. Xiao, *J. Anal. Appl. Pyrol.* **2016,** *119*, 147-156.
- **3.** H. Kobayashi, M. Yabushita, T. Komanoya, K. Hara, I. Fujita, A. Fukuoka, *ACS Catal.* **2013,** *3*, 581-587.
- **4.** G. Fan, Y. Wang, Z. Hu, J. Yan, J. Li, G. Song, *Carbohydr. Polym.* **2018**, 200, 529-535.
- 5. D. Theng, N.-E. El Mansouri, G. Arbat Pujolràs, B. Ngo, M. Delgado Aguilar, M. À. Pèlach Serra, P. Fullana i Palmer, P. Mutjé Pujol, *Bioresources* 2017, 12, 2379-2393.
- **6.** C. A. Gasser, G. Hommes, A. Schäffer, P. F.-X. Corvini, *Appl. Microbiol. Biotechnol.* **2012,** *95*, 1115-1134.
- Q. Chen, T. Ren, Y. Chai, Y. Guo, I. D. V. Ingram, M. North, H. Xie, Z. K. Zhao, *ChemCatChem* 2018, 10, 5377–5381.
- 8. S. D. Mansfield, H. Kim, F. Lu, J. Ralph, Nat. *Protoc.* **2012**, *7*, 1579-1589.
- 9. A. J. Ragauskas, G. T. Beckham, M. J. Biddy, R. Chandra, F. Chen, M. F. Davis, B. H. Davison, R. A. Dixon, P. Gilna, M. Keller, *Science* 2014, 344, 1246843.
- **10.** R. Rinaldi, R. Jastrzebski, M. T. Clough, J. Ralph, M. Kennema, P. C. Bruijnincx, B. M. Weckhuysen, *Angew. Chem. Int. Ed.* **2016**, *55*, 8164–8215.
- **11.** Y. Zhou, Q. Zeng, H. He, K. Wu, F. Liu, X. Li, *Green Energy Environ*. **2024**, *9*, 114–125.
- 12. Li, K.; Yu, S.; Li, Q.; Zhang, Y.; Zhou, H. Front. *Chem. Sci. Eng.* 2024, 18, 50.
- **13.** W. Zhang, J. Chen, R. Liu, S. Wang, L. Chen, K. Li, *ACS Catal.* **2021**, *11*, 5327–5337.
- **14.** Z. Shen, G. Zhang, C. Shi, J. Qu, L. Pan, Z. Huang, X. Zhang, J.-J. Zou, *Fuel* **2023**, *339*, 126634.
- 15. J. Bai, Y. Zhang, X. Zhang, C. Wang, L. Ma, ACS Sustainable Chem. Eng.2021, 9, 7706–7715

- **16.** B. Yu, G. Fan, S. Zhao, Y. Lu, Q. He, Q. Cheng, J. Yan, B. Chai, G. Song, *Appl. Biol. Chem.* **2021**, *64*, 1-13.
- 17. K. Li, J. W. Frost, J. Am. Chem. Soc. 1998, 120, 10545-10546.
- **18.** Shen, X.; Meng, Q.; Mei, Q.; Liu, H.; Yan, J.; Song, J.; Tan, D.; et al. *Chem. Sci.* **2020**, *11*, 1347–1352.
- **19.** J. Bai, Y. Zhang, X. Zhang, C. Wang, L. Ma, *ACS Sustainable Chem. Eng.* **2021,** *9*, 7112–7119.
- 20. Q. Chen, T. Ren, Y. Chai, Y. Guo, I. D. V. Ingram, M. North, H. Xie, Z. K. Zhao, *ChemCatChem* 2018, 10, 5377–5381.